Physics Department. Annual progress report 1 January - 31 December 1975

Research Establishment Risø, Roskilde

Publication date:
1975

Document Version
Publisher's PDF, also known as Version of record

Risø Report No. 334

Risø Report No. 334

Danish Atomic Energy Commission

Research Establishment Risø

Physics Department
Annual Progress Report

1 January - 31 December 1975

December 1975

Sales distributors: Jul. Gjellerup, 87, Sølvgade, DK-1307 Copenhagen K, Denmark

Available on exchange from: Library, Danish Atomic Energy Commission, Risø, DK-4000 Roskilde, Denmark

UDC 53

December 1975 Risø Report No. 334

Danish Atomic Energy Commission

Research Establishment Risø

PHYSICS DEPARTMENT

ANNUAL PROGRESS REPORT

1 January - 31 December 1975

edited by

H. Bjerrum Møller and B. Lebech

This report contains unpublished results and should not be quoted without permission from the authors.

ISBN 87-550-0368-0

PREFACE

The research work in the Physics Department at Risø covers four main fields:

Solid-State Physics (Neutron Scattering)
Plasma Physics
Nuclear Spectroscopy
Meteorology

The principal activities in these fields are presented in this report covering the period from 1 January to 31 December 1975.

An introduction to the work in each of the main fields is given in the respective sections of the report.

CONTENTS

		PAGE
Preface		3
1.	Solid State Physics (Introduction)	9
1.1.	The Cold Neutron Source at DR3	11
1.2.	The Magnetic Structure of Tb-Tm Alloys	12
1.3.	Theory of Random Anisotropic Magnetic Alloys	14
1.4.	Magnetic Properties of $CrNbO_4$ and $FeTaO_4$	15
1.5.	The Nuclear and Magnetic Structure of $MnNb_2O_6$	16
1.6.	Magnetic Excitations in Pr Metal	17
1.7.	Magnetic Excitations in Pr-5% Nd	18
1.8.	Inelastic Neutron Scattering from Ce under Pressure	18
1.9.	Theoretical Investigation of the Exchange Interaction in the Heavy Rare Earths	21
1.10.	Bose-Operator Expansions of Tensor Operators	22
1.11.	Absence of Giant Two-ion-anisotropy in the Heavy Rare Earth Metals	22
1.12.	Coherent Potential Approximation for Rare Earth Alloys	23
1.13.	Theory of the Temperature Dependence of Elastic Constants in Rare Earth Metals and Compounds	24
1.14.	Tables of Products of Tensor Operators and Stevens Operators	24
1.15.	Crystal Fields in Dilute Alloys of Rare Earths in Sc, Y, and Lu	24
1.16.	Spin Wave Dispersion in $CoCl_2$-$2D_2O$: A System of Weakly Coupled Ising Chains	25
1.17.	Magnon-Phonon Hybridization in $FeCl_2$	26
1.18.	Wave Vector Dependence of the Jahn-Teller Interaction in $TmVO_4$	27
1.19.	Magnetic Excitations and Critical Scattering in Pr_3Tl	29
1.20.	Elastic Magnetic Scattering in Pr Metal	30
1.21.	Critical Neutron Scattering in EuO	30

PAGE

1.22. Critical Fluctuations in the Dipolar-Coupled Ising Ferromagnet $LiTbF_4$..... 32
1.23. Critical Fluctuations in a Two-Dimensional, Site Random Antiferromagnet $Rb_2(Mn_{0.5}Ni_{0.5})F_4$.. 33
1.24. Critical Fluctuations in Tb with the Spiral Phase Suppressed by a Magnetic Field..... 34
1.25. Soft Mode Studies in Chloranil..... 34
1.26. Neutron Scattering Studies on CsDA and DCsDA... 35
1.27. High Pressure Structural Transitions in C_6D_6 and $C_{10}D_8$..... 36
1.28. The Solid to Liquid Phase Transition..... 37
1.29. Neutron Scattering Study of Transitions to Convection and Turbulence in a Nematic Liquid.. 38
1.30. Canonical Band Theory of the Volume and Structure Dependence of the Magnetic Moment of Fe..... 39
1.31. Spin Density of Pd_3Fe..... 40
1.32. Electronic Structure of Na-W Bronzes..... 41
1.33. Electronic Structure and Magnetic Breakdown in Ti..... 41
1.34. Temperature Dependence of the Lattice Dynamics of ^7Li..... 42
1.35. Neutron Scattering in C_2F_6..... 43
1.36. Structure and Dynamics of Monolayers of H_2 and D_2 Adsorbed on Grapnite..... 44
1.37. Dynamics of H_2 Adsorbed on Al_2O_3..... 45
1.38. Mosaic Structure of Single Crystals Studied by γ-Ray Diffraction..... 46

2. Plasma Physics (Introduction)..... 49

2.1. Secondary Electrons from Solid H_2 and D_2..... 49
2.2. Reflection of Energy from Solid Targets Bombarded with keV Protons..... 51
2.3. Theory of a Refuelling Pellet..... 52
2.4. Electron Temperature Measurements by Laser Scattering..... 52

PAGE

2.5. Pellet-Rotating Plasma Spectroscopy..... 52
2.6. Rotating Plasma Characteristics Determined by Measurements of Charge Exchange Neutrals and Doppler Broadening..... 53
2.7. Ion Acoustic Waves Propagating along a Density Gradient..... 54
2.8. Observation of Ion-Beam-Excited Electrostatic Ion Cyclotron Waves (eicw)..... 55
2.9. Stability Limits of the Ion-Beam-Excited Electrostatic Ion Cyclotron Instability..... 55
2.10. Ion Acoustic Waves in the Presence of High Frequency Electron Oscillations..... 56
2.11. Electromagnetic Radiation Originating from Unstable Electron Oscillations..... 56
2.12. Propagation Properties of Density Pulses in an Ion-Beam Plasma..... 57

3. Nuclear Spectroscopy..... 59

3.1. An Attempt to Form the ^{236}U Fission Isomer with Thermal Neutrons..... 59
3.2. Fine Structure in the Mass Distribution for Fission Fragments..... 60

4. Meteorology (Introduction)..... 63

4.1. Flow Over Non-Uniform Terrain..... 64
4.2. Stress-Profile Experiment..... 65
4.3. Simulation of Atmospheric Turbulence..... 66
4.4. Numerical Modelling of the Planetary Boundary Layer..... 67
4.5. Air-Sea Interaction (JONSWAP-1975)..... 68
4.6. Air-Sea Interaction (Kattegat 1975)..... 71
4.7. Climatology of Wind Direction Fluctuations.... 71
4.8. Climatology in Greenland..... 72
4.9. Time Series Analysis..... 73
4.10. Development of an Automatic Weather Station (AWS)..... 75

PAGE

4.11. Over-speeding in Cup Anemometers..... 76
4.12. Acoustic Sounder..... 77
4.13. Cold-Wire Technique..... 78
4.14. Dynamic Wind Loading..... 80
4.15. Applied Meteorology I: Site Evaluation..... 82
4.16. Applied Meteorology II: Air Pollution Studies... 83

5. Liquid N_2 and He Plant..... 84

6. Educational Activities and Publications..... 85

7. Staff of the Physics Department..... 105

1. SOLID STATE PHYSICS

The purpose of the work in solid state physics is to contribute to the fundamental understanding of the physical properties of condensed matter.

Neutron beams have properties that make them a unique tool for studies of solids and liquids on the microscopic level. For such investigations, the staff of the solid state physics section utilize thermal and cold neutrons from the DR 3 reactor, where five triple-axis spectrometers and one double-axis spectrometer are available. In three of the four tangential through-tubes of the reactor, a water scatterer placed close to the reactor core scatters a beam of thermal neutrons out through the tube to the spectrometers. A liquid hydrogen cold source (1.1) was installed in the fourth tangential tube in the spring of 1975. This provides two of the spectrometers with beams of cold neutrons. It is planned to install a neutron conducting tube from the cold source to an experimental hall during the fall of 1976. The section has a γ-ray diffractometer (1.38) for studies of the mosaic structure of crystalline samples.

The experimental and theoretical work may be roughly divided into the following main subject fields: Investigation of the static (1.2-1 5) and dynamic (1.6-1.19) properties of magnetic solids; studies of various kinds of phase transitions in solids and liquid-like systems (1.20-1.29); electronic energy band calculations of metals (1.30-1.33); and investigations of the structure and lattice dynamics of molecular crystals and adsorbed monolayers (1.34-1.37).

Studies of magnetism are to a large extent concentrated on the rare earth metals and alloys; for example, an experimental and theoretical investigation of the magnetic structures of random magnetic alloys (1.2-1.3), and a determination of the exchange parameters and the crystal field parameters of rare earth metals and alloys (1.6-1.15). It was shown that the previously reported large two-ion anisotropy of some of the heavy rare earth metals can be interpreted solely in terms of single-ion anisotropy, if a

new self-consistent Bose operator expansion of tensor operators is used instead of the usual Holstein-Primakoff transformation (1.10-1.11). Several other magnetic compounds were investigated (1.4-1.4 and 1.16-1.18), among these a magnetic salt (1.16) in which the dominant super-exchange couples the magnetic ions in strands along a crystallographic axis. The spin wave dispersion measured for this compound was interpreted by a simple model of weakly coupled Ising chains.

Magnetic properties were calculated for a number of 3d-transition metals (1.30-1.33) by means of a fast computational method of calculating electronic energy bands from canonical bands and potential parameters.

Investigations were made of the fundamental characteristics of various kinds of phase transitions, such as magnetic (1.19-1.24), structural (1.25-1.27), and hydrodynamic phase transitions (1.29), and melting (1.28). In particular, magnetic phase transitions were investigated in singlet - ground-state systems (1.19-1.20), in a ferromagnetic insulator (1.21), in a dipolar-coupled Ising ferromagnet (1.22), and in two-dimensional random antiferromagnets (1.23), while studies of the structural phase transition were centered on transitions in molecular crystals. The hydrodynamic transitions (1.29) to convection and turbulence were studied by coherent elastic neutron diffraction in the nematic phase of a liquid crystal. A central mode was observed at the magnetic transition in singlet - ground-state systems (1.19-1.20) and at the structural phase transition in a molecular crystal (1.25).

Investigations of the structure and dynamics of adsorbed monolayers (1.36-1.37) revealed that the monolayer structure exists over a wide range of densities of adsorbed hydrogen and deuterium molecules. Moreover, it appeared that molecules adsorbed on graphite are free rotators, whereas the rotational energy of ortho-molecules adsorbed on aluminium oxide is partly quenched.

1.1 The Cold Neutron Source at DR3

The cold source became operational in March 1975. It consists of a 150 cm^3 moderator chamber filled with supercritical H_2 (15.5 atm at 30 K) installed in one of the tangential beam tubes. The beam holes at each end of the tube are presently equipped with triple-axis spectrometers (TAS I and TAS VI).

The performance of the cold source was evaluated on the basis of measurements of the monochromatic neutron fluxes at the sample positions of these spectrometers. As can be seen from Fig. 1, considerable gain has been achieved in comparison to the normal water sources. It is particularly encouraging that there is a gain over a wide neutron energy range up to 20 meV, which includes the often-used energies around 15 meV. It appears that the

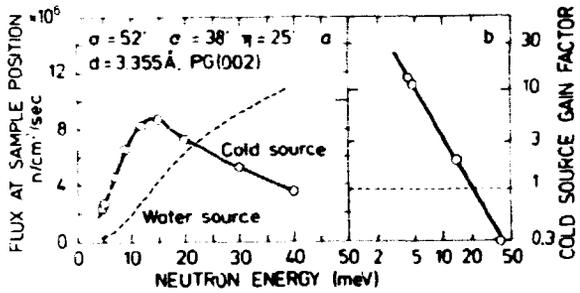

Fig. 1. a) Monochromatic fluxes at the sample position of TAS I obtained with a curved graphite moncchromator. b) The gain in monochromatic neutron flux from the cold source as compared to the flux from the normal water source.

cold source spectrum is quite insensitive to changes in the moderator temperature up to 45 K, making the experiments conveniently independent of normal cold source operations. The source has operated very reliably since installation and numerous experimental studies have benefited from the improved flux of cold neutrons, especially below the Be-filter cut-off at 5 meV. These studies include:

Critical scattering in EuO

Jahn-Teller transition in $TmVO_4$

Dynamics of D_2 and H_2 adsorbed on grafoil and on Al_2O_3

Critical scattering in $LiTbF_4$
Excitation and magnetic ordering in Pr and Pr-5% Nd
Critical Scattering in Pr_3Tl
Soft phonon structural transition in Chloranil
Magnon-phonon coupling in $FeCl_2$
Nuclear and electronic magnetic ordering in $HoPO_4$
Spin-wave lifetimes in Tb
Crystal field excitons in Pr_3Te_4
Magnetic excitation in the mixed crystal Mn/ZnF_2

Most of these investigations would have been impractical if performed on normal water-source spectrometers.

1.2 The Magnetic Structure of Tb-Tm Alloys

(P. A. Hansen, P. Fynbo (The Technical University of Denmark), and B. Lebech)

One reason for the interest in the magnetic structure of the heavy rare earth alloys is to determine whether the spins of the constituents forming the alloy order magnetically with the same easy plane or axis as that of the separate elements, or if the anisotropy aligns the spins of the constituents and forms a homogeneous magnetic structure. The Tb-Tm alloy system is particularly suited to elucidate this problem because the magnetic moment of Tb is constrained to the basal plane by large anisotropy forces and a large axial anisotropy constrains the Tm moments to lie along the c-axis.

Figure 2 shows the temperature dependence of the ordered moments for a Tb-55% Tm and a Tb-65% Tm alloy crystal. Just below the Néel temperature, the ordering is to a basal plane spiral ($\mu_\perp$). At lower temperatures a c-axis sine-modulated component ($A_{//}$) of the moment appears. At still lower temperatures this component becomes ferromagnetic ($\mu_{//}$). The data cannot be analyzed in terms of a homogeneous magnetic structure since the total moment, μ_T, at low temperatures calculated from the data as $\mu_T = \sqrt{\mu_\perp^2+\mu_{//}^2}$, is lower than the expectation value of μ for pure Tb and pure Tm. Thus, in contrast to previous measurements on other rare earth

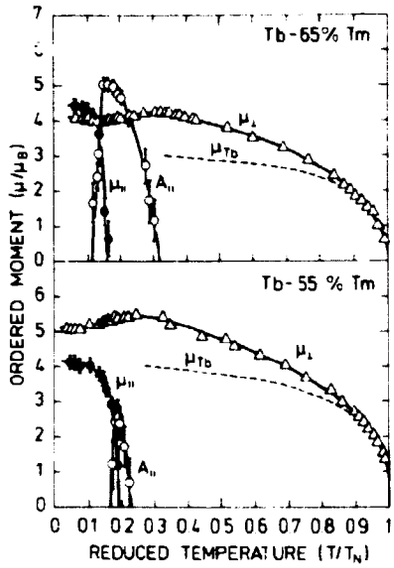

Fig. 2. The magnetic moment parallel ($\mu_{\parallel}$) and perpendicular ($\mu_{\perp}$) to the c-axis for Tb-55% Tm and Tb-65% Tm as a function of reduced temperature. $A_{\parallel}$ is the amplitude of the modulated c-axis component. μ_{Tb} is the magnetic moment as measured on pure Tb and scaled by the concentration. The difference between $\mu_{\perp}$ and μ_{Tb} at high temperature is presumably due to a small polarization of the Tm spins caused by the order of the Tb moments.

alloys [1], the present neutron diffraction measurements on Tb-Tm single crystal alloys show unambiguously that a inhomogeneous phase exists in these alloys. In this phase, Tb-spins lie in the basal plane while the Tm-spins lie along the hexagonal c-axis. The magnetic structure of a Tb-40% Tm alloy is similar to that of the Tb-55% Tm and the Tb-65% Tm, but the phase in which the c-axis component oscillates has vanished. Tb-12% Tm has a magnetic structure similar to that of pure Tb, and it is expected that Tm rich alloys will have an initial ordering along the c-axis similar to that observed in pure Tm and an inhomogeneous phase at low temperature. So far attempts to grow crystals with a Tm content of ∿90% have failed.

Preliminary calculations of the magnetic phase diagram based on a mean field theory (1.3), which includes only single-ion anisotropy and isotropic exchange interactions, have shown overall agreement with these measurements [2].

---

[1] A. H. Millhouse and W. C. Koehler, Int. J. Magnetism 2, 389 (1971) and references therein.

[2] P.-A. Lindgård, Theory of Random Anisotropic Magnetic Alloys. Submitted to Phys. Rev.

1.3 Theory of Random Anisotropic Magnetic Alloys

(P.-A. Lindgård)

A mean field-crystal field theory was developed for random, multi-component, anisotropic magnetic alloys. It is especially applicable to rare earth alloys. The theory may be used to study multicritical points and phase transitions between various states characterized by order parameters with different spatial directions or different ordering wave vectors. Thus, theoretical predictions can be made of the phase diagrams and magnetic moments, based on known parameters for the rare earth alloys. The results for Nd-Pr, pure dhcp Nd, Tb-Er and Tb-Tm alloys, agree qualitatively with experimental observations. A comparison of the theoretical and experimental results for the Tb-Er alloys are shown in Fig. 3. In order to reduce the number of parameters in the calculation to three, the parameters were obtained by assuming de Gennes scaling to be valid for the exchange inter-

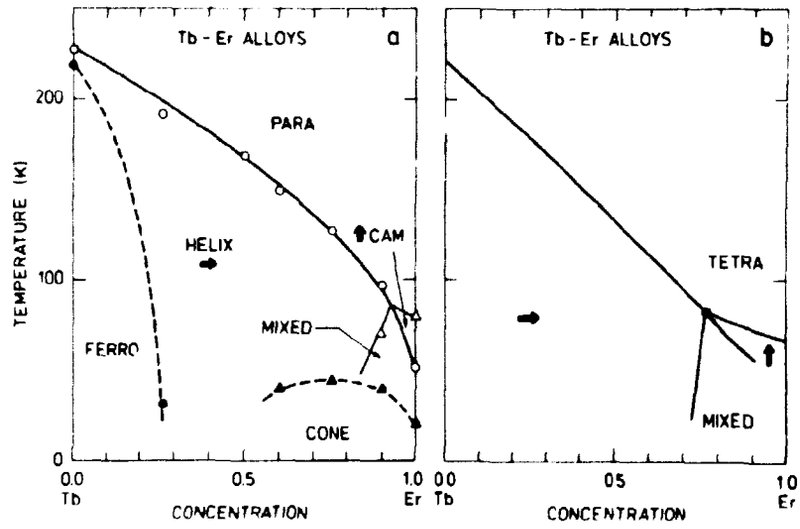

Fig. 3. a) The experimental phase diagram for the Tb-Er alloys by Millhouse and Koehler [3]. The full line indicates a second-order transition, the broken line a first-order transition. b) The calculated phase diagram for the Tb-Er alloys obtained by scaling by the de Gennes and the Stevens factors and with the Tb-Tb exchange parameters adjusted to give the correct Néel temperature for pure Tb. The first-order transitions to the ferromagnetic structures were not considered.

[3] A. H. Millhouse and W.C. Koehler, Les Element des Terres, Paris, Colloque Intern. CNRS No. 180 Paris 2, 214 (1970).

actions (Tb-Tb, Tb-Er, and Er-Er) and by the Stevens factor scaling for the anisotropy constants. The relatively good agreement shows that this procedure is essentially correct. To obtain better agreement, the Tb-Er exchange interaction in particular has to be increased. A similar conclusion may be made for the Tb-Tm alloy system (1.2).

1.4 Magnetic Properties of $CrNbO_4$ and $FeTaO_4$

(B. Lebech, A. Nørlund Christensen (University of Aarhus, and T. Johansson (The Technical University of Denmark))

According to X-ray powder investigations, the compounds $CrNbO_4$ and $FeTaO_4$ can crystallize with structures of the rutile type. Rutile crystallizes in the tetragonal space group $P4_2/mnm$ with the metal atoms in 2a, and the oxygen atoms in 4f. For octahedral coordination, the ionic radii of the metal ions (Cr^{3+}, Fe^{3+}, Nb^{5+}, and Ta^{5+}) are almost equal and it is therefore likely that the metal ions of these compounds are randomly distributed in the 2a position of the rutile structure.

Neutron powder diffraction at 300, 77, and 4.8 K confirmed that $CrNbO_4$ has such a random rutile structure. The anomaly observed in the susceptibility at 9.3 K is thus caused by a spin glass transition. The cusp in the susceptibility of $CrNbO_4$ may be described by the molecular field calculations of Sherrington [4] and Southern [5]. Neutron powder diffraction at 300, 77, and 8 K have further shown that $FeTaO_4$ has the trirutile structure ($Fe(Fe_{0.25}Ta_{0.75})_2O_6$) in which two-thirds of the Fe ions are ordered at sites 2a and the remaining metals ions are randomly arranged at sites 4e. The transition at 25 K observed in the susceptibility at low magnetic fields is of spin glass nature. Below 25 K, the spins of the ordered Fe-atoms (2a) are magnetically ordered in clusters with a size of 10-20 unit cells, whereas the spin glass behaviour originates from the random Fe-ions (4e). The Mössbauer spectrum of $FeTaO_4$ [6] at 4.2 K contains the characteristics of the spectrum of a magnetically ordered compound and resembles the Mössbauer spectra of AuFe dilute alloys below the spin glass trans-

[4] D. Sherrington, J. Phys. C: Solid State Phys. 8, L208 (1975).
[5] B. Southern, J. Phys. C: Solid State Phys. 8, L212 (1975).
[6] N. A. Fadeeva et al., J. Phys. Paris 32, C1, 503 (1971).

ition. The Mössbauer data thus agree with both the spin glass nature of $FeTaO_4$ and with the observed magnetic short-range order of the ordered Fe-ions in $FeTaO_4$.

1.5 The Nuclear and the Magnetic Structure of $MnNb_2O_6$

(B. Lebech, O. V. Nielsen (The Technical University of Denmark), and F. Krebs Larsen (University of Aarhus))

$MnNb_2O_6$ has the orthorhombic columbite structure (space group Pbcn) with four formula units per unit cell. A neutron diffraction study was made of the nuclear and the magnetic structure of $MnNb_2O_6$ single crystals. The 13 nuclear parameters were determined from 304 reflections at room temperature. The magnetic ordering below $T_N = 4.4$ K was previously observed in powder diffraction experiments [7] and in measurements of the magnetoelectric and magnetic susceptibility [8]. Figure 4 shows the positions and numbering of the four Mn-ions in the unit cell. All possible antiferromagnetic structures may be regarded as a superposition of the types labelled $\bar{G}$, $\bar{A}$ and $\bar{C}$ [9], where

$$\bar{G} = \bar{\mu}_1 - \bar{\mu}_2 + \bar{\mu}_3 - \bar{\mu}_4$$
$$\bar{A} = \bar{\mu}_1 - \bar{\mu}_2 - \bar{\mu}_3 + \bar{\mu}_4$$
$$\bar{C} = \bar{\mu}_1 + \bar{\mu}_2 - \bar{\mu}_3 - \bar{\mu}_4$$

and $|\bar{\mu}_1| = |\bar{\mu}_2| = |\bar{\mu}_3| = |\bar{\mu}_4| = \mu$.

The magnetic structure proposed from the powder data is a colinear G_{xz}-type, where the z-(c-axis) components of the moments amount to ∿17% of the x-(a-axis) components, but the powder diffraction data fail to disclose minor deviations from this model. The present neutron diffraction study on single crystals shows that the antiferromagnetic structure at 1.2 K is a superposition of G- and A-type structures of the form $0.90\ \bar{G}_x + 0.34\ \bar{G}_y + 0.28\ \bar{A}_z$. The corresponding space group is $P2_1'/c$. The moment directions are shown on Fig. 4. If the magneto-electric tensor is examined in

---

7) H. Weitzel, Z. Anorg. Allg. Chem. 119 (1971).

8) L. M. Holmes et al., Solid State Commun. 11, 409 (1972).

9) E. F. Bertaut, Magnetism Vol. III, Chap. 4, New York and London Academic Press (1963).

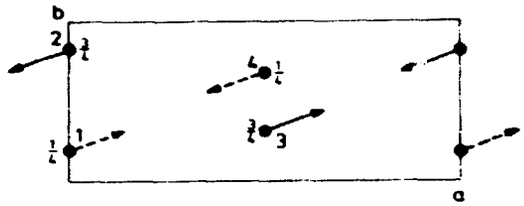

Fig. 4. Positions and numbering of the Mn-ions in the unit cell of $MnNb_2O_6$. Also shown are the ion moment directions of the antiferromagnetic structure determined from neutron diffraction on single crystals. Full and dashed arrows indicate that the moment is directed upwards or downwards, respectively.

terms of the G_{xy}-A_z type structure determined from the single crystal data, we find that the magneto-electric tensor $\overline{\overline{\alpha}}$ may have four non-vanishing components, α_{xz}, α_{yz}, α_{zx}, and α_{zy}. These results are consistent with the magneto-electric study [8] in which non-vanishing α_{yz} and α_{zy} components were found.

1.6 Magnetic Excitations in Pr Metal

(J. G. Houmann, A. R. Mackintosh, B. D. Rainford (Imperial College, London, U.K.), O. D. McMasters*, and K. A. Gschneidner, Jr.*, (*Iowa State University, U.S.A.))

Measurements of the magnetic excitation energies in Pr metal [10]

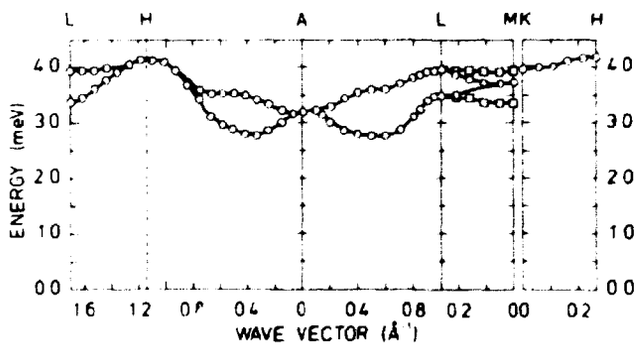

Fig. 5. Dispersion relations for the magnetic excitations in Pr along the zone boundary lines at 4.2 K. The solid lines are guides for the eye.

---

[10] J. G. Houmann, M. Chapellier, A. R. Mackintosh, P. Bak, O. D. McMasters, and K. A. Gschneidner, Jr., Phys. Rev. Lett. 34, 587 (1975).

were continued and the energies of the excitations on the hexagonal sites along most of the boundaries of the Brillouin zone are now measured (Fig. 5). It is seen that two-ion anisotropy generally splits the degeneracy of the J_x and J_y excitations predicted by the model so far used in the analysis. A more complete analysis is in progress and it is expected that the additional results will allow a complete determination of the interatomic exchange parameters.

1.7 Magnetic Excitations in Pr-5% Nd

(J. G. Houmann, W. J. L. Buyers (Chalk River, Canada), A. R. Mackintosh, O. D. McMasters*, and K. A. Gschneidner, Jr.* (*Iowa State University, U.S.A.))

A study of the temperature dependence of the magnetic excitations in Pr [10] led to an interest in investigating a similar system with a finite ordering temperature, and therefore a study of Pr-5% Nd alloy [11] was initiated. The crystal used in the experiment was small and presumably not single, and the intensity obtained from the cold-source triple-axis spectrometers at 5 meV was hardly sufficient to obtain reliable statistics. However, we did observe neutron groups at 8.5 K that are consistent with previous observations in Pr. In addition, we observed extra scattering at energies below and above the energies of the Pr groups. At present it is uncertain whether this extra scattering is real or an effect of the crystal not being single. The observed neutron groups showed no marked temperature dependencies as the temperature was lowered to 1.3 K. The experiment is temporarily suspended while awaiting a larger single crystal.

1.8 Inelastic Neutron Scattering from Ce under Pressure

(B. D. Rainford (Imperial College, London, U.K.), B. Buras, and B. Lebech)

At room temperature fcc γ-Ce undergoes a first order isomorphic transition to the fcc α-phase at 7 kbar. However, samples which

---

11) B. Lebech, K. A. McEwen, and P.-A. Lindgård, J. Phys. C: Solid State Phys. 8, 1684 (1975).

contain mixtures of both phases at atmospheric pressure may be prepared. The intensity of the paramagnetic diffuse neutron scattering from samples containing preferably γ-Ce or α-Ce respectively at atmospheric pressure was first studied by Wilkinson et al.[12] Their results were interpreted in terms of a paramagnetic γ-phase with a localized magnetic moment originating from the 4f-electron and a non-magnetic α-phase with a Pauli-type paramagnetism. Since the 4f-level in α-Ce is just above the Fermi level it was suggested [13] that exchange enhancement may occur at the transition. The intensity of the paramagnetic inelastic scattering is proportional to the square of the magnetic moment and the width of the inelastic paramagnetic scattering depends on both the square of the magnetic moment and on the exchange integral. Therefore, if exchange enhancement occurs at the γ-Ce to α-Ce phase transition at 7 kbar, the width of the inelastically scattered neutrons centered at zero-energy transfer should vary. Recently the inelastic neutron scattering from Ce metal at atmospheric pressure was studied by Rainford [14]. The observed magnetic scattering had a large energy width characteristic of paramagnetic scattering from magnetic moments having a very rapid relaxation rate ($\sim 4\times10^{12}s^{-1}$). The relaxation was attributed to the conduction electrons and an estimate was made of the sf exchange interaction (J_{sf}).

We measured [15] the inelastic neutron scattering from Ce metal under pressure both below and above the γ-α transition using a sample of less than 1 cm^3 in volume in an aluminium oxide pressure cell. The results were not conclusive because of a large background scattering, and therefore another high pressure cell was made of a special Al-alloy. This cell has a sample volume of 10 cm^3 and holds pressures up to 8 kbar. The results at 300 K for the inelastic neutron scattering at atmospheric pressure, 6 kbar, and 8 kbar are shown on Fig. 6. A preliminary analysis in which the measured line shapes were fitted to three

---

12) M. K. Wilkinson et al., Phys. Rev. 122, 1409 (1961).

13) B. Coqblin, Colloque, CNRS, No. 180 Grenoble 2, 579 (1969).

14) B. D. Rainford, Thesis (1969).

15) B. Buras, B. Lebech, and B. D. Rainford, Risø Report No. 320, 55, (1974).

Lorentzians centered at zero energy transfer and at $\pm\Delta$, where Δ is the crystal field splitting, yielded Δ= 9.9 meV at 1 atmosphere in good agreement with previous measurements [15] and 10.7 meV at 6 kbar. The width of the Lorentzians increases by ∿28% from atmospheric pressure to 6 kbar. This suggests an increase

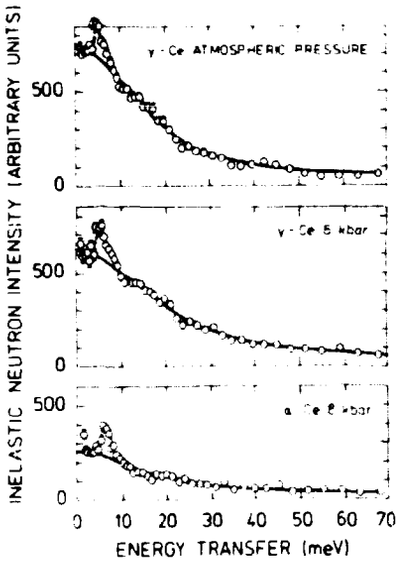

Fig. 6. Inelastic neutron scattering at 300 K from Ce-metal at 0, 6, and 8 kbar. The background scattering from the pressure cell has been subtracted from the data. The solid lines are the results of a least squares fit of the data to three Lorentzians in the γ-phase and one Lorentzian in the α-phase. The small peak at ∿6 meV is caused by a peak in the density of states and was subtracted from the data before the fits were made.

in the relaxation rate due to an increase of J_{sf} by ∿14%. This effect is smaller than the 40% predicted by Coqblin [13] from calculations based on the Schrieffer-Wolf transformation of the Anderson model for the f-states. The data for α-Ce at 8 kbar fit best to a single Lorentzian of width 13.4 meV. We suggest that this residual scattering in α-Ce is magnetic in origin. The total scattering is ∿38% of that observed in α-Ce below the phase transition.

To summarize, the paramagnetic inelastic scattering shows that there is a partial delocalization of the 4f electrons on going through the γ-α phase transition and that there is considerable magnetic scattering in the α-phase. We suggest that this is caused by spin fluctuations in the highly exchange-enhanced 4f band. From the intensity of the scattering we estimate that the occupation of the 4f band is about 0.38 electrons in α-Ce.

1.9 Theoretical Investigation of the Exchange Interaction in the Heavy Rare Earths

(J. F. Cooke and P.-A. Lindgård)

A numerical calculation of the indirect exchange integral, $J(\bar{q})$, in Gd was recently reported by Lindgård et al.[16]. Their result for the band width, $(J(0)-J(\bar{q}_{max}))$ was found to be roughly a factor of four larger than that found from neutron scattering experiments. If the calculated $J(\bar{q})$ is scaled by this factor, rather good overall agreement between theory and experiment can be obtained for all values of q although a systematic discrepancy still occurs at low $\bar{q}$. In order to investigate the source of these discrepancies, we carried out a derivation of $(J(0)-J(\bar{q}_{max}))$ for a ferromagnet based on a Green's function formalism. An expression for $J(\bar{q})$, which includes the enhancement of the indirect exchange resulting from interactions between the conduction electrons, was obtained within the Hartree-Fock approximation. The theory also generates energy band equations that include the 4f-conduction electron interaction in a self-consistent way. Furthermore, the formalism is well suited to calculate the damping of spin waves caused by the interaction of the spin waves with the conduction electrons.

Two possible sources may be suggested for the discrepancy between the previously calculated band width [16] and the band width determined from neutron scattering experiments. Firstly, rather large errors could result from inter-band contributions to $J(\bar{q})$ if the energy band equations are not solved self-consistently. A more correct treatment tends to reduce the difference between the measured and the calculated values of $(J(0)-J(\bar{q}_{max}))$. Secondly, preliminary numerical calculation has shown that the enhancement effect is important only in the low $\bar{q}$ region. Therefore, the enhancement effect may account for the systematic discrepancy in the low $\bar{q}$ behaviour of $J(\bar{q})$. Although additional numerical calculations are needed, it thus appears that the two effects mentioned above may account for a significant part of the difference between the theoretical and experimental values of $J(\bar{q})$ for Gd.

---

[16] P.-A. Lindgård, B. N. Harmon, and A. J. Freeman, Phys. Rev. Lett. 35, 383 (1975).

1.10 Bose-operator Expansions of Tensor Operators

(P. -A. Lindgård and A. Kowalska (Jagiellonian University, Cracow, Poland)

The matching-of-matrix-element method[17] was used to find a new self-consistent Bose operator expansion for tensor operators in spin systems with isotropic exchange interaction and anisotropy. Tables were derived for all tensor operators relevant to cubic and hexagonal symmetry. A discussion of renormalized spin wave theory for a system with planar anisotropy shows that the Goldstone theorem is rigorously fulfilled up to the considered order of perturbations. It can also be shown that the new expansion introduces wave-vector-dependent terms from the single-ion anisotropy into the dispersion relation.

1.11 Absence of Giant Two-ion-Anisotropy in the Heavy Rare Earth Metals [+]

(P.-A. Lindgård)

The Bose operator transformation of tensor operators (1.10) was used in a calculation of the spin waves in the heavy rare earth metals [18,19]. The resulting spin waves fulfil the Goldstone theorem exactly for planar anisotropy. The Er spin wave results for the cone phase were re-analyzed with an isotropic exchange interaction similar to that found in other rare earth metals plus a single-ion anisotropy. The Tb data may be interpreted within the same model. The resulting fit is shown in Fig. 7. The previously found large two-ion anisotropy[19] was caused by an inadequate treatment of the single-ion anisotropy leading to an incorrect expression for the spin wave dispersion.

[+] Work performed for the U. S. Energy Research and Development Administration under Contract No. W-7405-eng-82 during a visit to Iowa State University and Ames Laboratory, Iowa, U.S.A.

17) P.-A. Lindgård and O. Danielsen, J. Phys. C: Solid State Phys. 7, 1523 (1974).

18) J. Jensen, J. C. G. Houmann, and H. B. Møller, Phys. Rev. B12, 303 (1975).

19) R. M. Nicklow, et al., Phys. Rev. Lett. 27, 334 (1971).

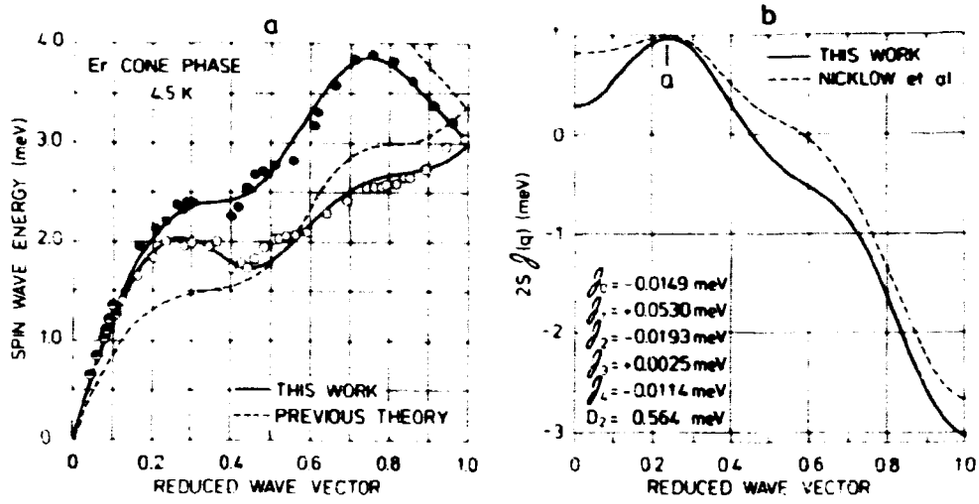

Fig. 7. a) The spin wave data for Er by Nicklow et al.[19]. The full line is the fit to the present theory using six parameters and a q-independent anisotropy. The dashed line is the best fit of the previous theories using eight parameters [19]. By introducing a q-dependent anisotropy a curve almost identical to the full line was obtained by Nicklow et al. with ten parameters. b) The deduced exchange interaction 2SJ(q). The dashed curve is shifted to give the same J(Q). The exchange parameters are given on the figure.

1.12 Coherent Potential Approximation for Rare Earth Alloys

(P.-A. Lindgård)

In the coherent potential approximation the frequency and wave vector dependent susceptibility of a binary alloy is found to be

$$\chi(q,\omega) = \frac{c(\frac{1}{\chi_2} + \Sigma_{12}) + (1-c)\ (\frac{1}{\chi_1} + \Sigma_{12})}{(\frac{1}{\chi_1}\frac{1}{\chi_2} - \Sigma_{12}^2)} .$$

where c is the concentration of element 1. The inverse enhanced susceptibility χ_n (n=1,2) of each element constituting the alloy is given by

$$\frac{1}{\chi_n} = \frac{1}{\chi_n^o} - \Sigma_{nm}(q,\omega,c)$$

in terms of the crystal field susceptibility χ_n^o and the self energies $\Sigma_{nm}(q,\omega,c)$. The neutron scattering from excitations

in such an alloy is related to $\mathrm{Im}(\chi(q,\omega))$. The static properties are related to $\chi(Q,0)$, where Q is the ordering wave vector.

1.13 Theory of the Temperature Dependence of Elastic Constants in Rare Earth Metals and Compounds

(P.-A. Lindgård and B. Lüthi (Rutgers College, New Jersey, U.S.A.))

The elastic constants in a magnetic material with magneto-elastic interactions depend on the thermal population of the magnetic (crystal field) states. The elastic constant may be thought of as a susceptibility function for strains. The strains can be expanded in terms of tensor operators $\mathcal{O}_{\ell m}$, with ℓ even, the simplest being the quadrupole moment operator. The magnetic susceptibility is a function of $\mathcal{O}_{\ell m}$ operators with ℓ=1 only. Previously only the ℓ=2 terms were considered for the strain susceptibility. The strain susceptibilities have now been calculated for ℓ = 2, 4, and 6 and an analysis made of the temperature variation of the elastic constants in the rare earth pnictides. The data for dhcp Pr and Nd have also been analyzed.

1.14 Tables of Products of Tensor Operators and Stevens Operators

(P.-A. Lindgård)

Numerical tables of products of tensor (Racah) operators, $R_{\ell m}(J)$, and Stevens operators, $O_\ell^m(J)$, working with a J-multiplet were calculated as a function of $X = J(J+1)$ [20]. All values of ℓ and m up to six are included. The tables may be used to calculate for example commutation relations and thermal averages.

1.15 Crystal Fields in Dilute Alloys of Rare Earths in Sc, Y and Lu

(O. Rathman and P. Touborg (University of Odense))

The crystal field levels in Sc-2 at% Er, Lu-2 at% Er and Y-1 at% Dy have been studied by inelastic neutron scattering. The spectra for

---

[20] P.-A. Lindgård, Risø Report No. 313 (1974) and J. Phys. C: Solid State Phys. 8, 3401 (1975).

[21] O. Rathman, J. Als-Nielsen, P. Bak, J. Høg, and P. Touborg, Phys. Rev. B10, 3983 (1974).

[22] J. Høg and P. Touborg, Phys. Rev. B9, 2920 (1974) and Phys. Rev. B11, 2660 (1975).

Sc-Er and Lu-Er alloys are rather similar to the spectra obtained for Y-Er [21] and they are in agreement with the crystal field level schemes deduced from bulk magnetization measurements [22]. The results of the inelastic neutron scattering from the Y-Dy alloy disagreed with these level schemes and it was thus apparent that a correction allowing for magnetic ordering was necessary. Neutron diffraction showed that ordered regions were present up to relatively high temperatures which may change the initial susceptibility drastically. However, the correct paramagnetic susceptibility for the Y-Dy alloy was obtained from isothermal magnetization curves and the crystal field parameters were redetermined from fits to the proper initial susceptibilities. These new crystal field parameters are in agreement with the inelastic neutron scattering spectra.

When comparing the new crystal field parameters, B_{ij} divided by the corresponding Stevens factors, α, β, and γ determined for a given rare earth impurity, we find that within the experimental errors the values of B_{40}/β, B_{60}/γ, and B_{66}/γ are independent of the host. As expected, B_{20}/α varies with the c/a-ratio throughout the series of alloys investigated because the c/a-ratio is close to but not ideal. In contrast to the previous analysis the values of B_{20}/α determined for the Y-Er and the Y-Dy agree within the experimental errors. This gives confidence that the crystal field parameters for a pure magnetic rare earth can be extracted from the crystal field parameters determined for the dilute alloys.

1.16 Spin Wave Dispersion in $CoCl_2$-$2D_2O$: A System of Weakly-Coupled Ising Chains

(J. K. Kjems, J. Als-Nielsen and H. Fogedby (ILL Grenoble, France))

$CoCl_2$-$2D_2O$ is a magnetic salt in which the dominant super-exchange interaction couples the Co^{2+} ions in strands along the crystallographic c-direction. The interactions are anisotropic so the Ising model gives a good description of the magnetic properties. This was clearly demonstrated by infrared absorption measurements [23] as functions of external magnetic field and temperature in the various magnetically-ordered phases.

---

[23] J. B. Torrance, Jr. and M. Tinkhan, Phys. Rev. 187, 587 (1969).

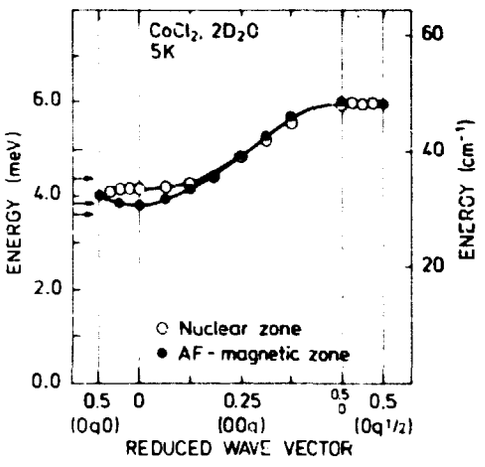

Fig. 8. Observed dispersion of the one-magnon excitations in $CoCl_2$-$2D_2O$ along two directions in the reciprocal space.

Inelastic neutron scattering [24] was used to study the magnetic excitation spectrum as function of wave vector in the antiferromagnetic phase (ferromagnetic along the Co^{2+} chains) at zero applied field. The observed dispersion is shown in Fig. 8. The results may be interpreted in terms of a simple model that relates the average energy to the Ising part of the interaction and the overall dispersion to the transverse exchange, and in which the splitting between spin waves pertaining to different sublattices is caused by the transverse anisotropy. The detailed, quantitative analysis results in somewhat different values for the exchange parameters than can be inferred from optical data alone.

1.17 Magnon - Phonon Hybridization in $FeCl_2$

(J. G. Houmann and K. Ziebeck (ILL, Grenoble, France))

$FeCl_2$ is an example of a two-dimensional ferromagnet with a large single-ion anisotropy. It is composed of hexagonal sheets of ferromagnetically aligned Fe^{2+}-ions with the strong anisotropy confining the moments to the hexagonal c-axis. A very weak antiferromagnetic coupling exists between the hexagonal planes, so the overall magnetic structure is antiferromagnetic with a Néel temperature of 23.5 K. A magnon-phonon coupling involving only the transverse acoustic phonons is expected in $FeCl_2$ [25].

---

24) J. K. Kjems, J. Als, Nielsen, and H. Fogedby, Phys. Rev. B12, 5190 (1975).

25) S. W. Lovesey, J. Phys. C: Solid State Phys. 7, 2049 (1974).

The separation of the hybridization excitations at the nominal intersection of the magnon and transverse phonon is only ∿0.3 meV and, moreover, the non-interacting magnon lies approximately midway between the hybridized modes. A magnetic field applied parallel to the c-axis increases the separation of the modes because it lifts the degeneracy of the magnon excitations. This eases the observation of the interactions by means of neutrons.

An experiment was undertaken at the cold-source triple-axis spectrometer to observe the magnon-phonon interaction. The analyzer was kept fixed at an energy of 5 meV giving an energy resolution of 0.18 meV. A Be filter was inserted in the beam in front of the analyzer in order to eliminate contamination from higher-order neutrons. The sample was placed in a super conducting magnet. Preliminary measurements indicate that the splitting can be observed even in zero field, that the degeneracy of the magnon excitations is lifted and that the splitting is increased when a magnetic field is applied. However, the crystal used in the experiment is rather poor. Furthermore, we had to work with an unfavourable crystal orientation ((100) and (105) in the scattering plane) in order to compromise between the two requirements of having a sizable c-axis component of a vertical field and a non-vanishing magnetic structure factor. This crystal orientation resulted in severe absorption problems. Therefore, only very poor statistics were obtained in the observed neutron groups. The experiment will be continued when a more suitable crystal is available.

1.18 Wave-vector Dependence of the Jahn-Teller Interactions in $TmVO_4$

(J. K. Kjems, W. Hayes*, and S. H. Smith*(*University of Oxford, U. K.))

The co-operative Jahn-Teller effect is the driving mechanism for many of the structural phase transitions that occur in rare earth (RE) insulators [26]. The RE-vandadates have been the most extensively studied. Here, the experimental evidence collected by a variety of experimental techniques, such as ultrasonics,

---

[26] G. A. Gehring and K. A. Gehring, Rep. Prog. Phys. 38, 1 (1975).

Raman, Brillouin, fluorescence and X-ray spectroscopy, can be understood within the framework of a simple, linear, random phase approximation theory devised by Elliot et al.[27]. $TmVO_4$ has proved to be the simplest model compound with a doubly degenerate electronic ground state of the Tm^{3+} ions that is well separated from the other levels of the $^3H_4$-multiplet. At T_D = 2.1 K, the degeneracy is lifted mainly because of the interaction with acoustic strains, and the crystal undergoes an orthorhombic distortion. The degeneracy can also be lifted by means of a magnetic field along the tetragonal axis. This suppresses the structural transition in analogy to a transverse field in the Ising model. However, the coupling to the acoustic phonon remains and it can be probed by inelastic neutron scattering. Such measurements were performed [28] in fields up to 50 k0e and the observed anticrossing between the B_{2g} acoustic phonon propagating in the basal plane and the Zeeman split electronic ground state doublet is seen in Fig. 9. As the field is increased, the crossing point moves out into the Brillouin zone, and hence one can directly measure the strength of the interaction as a function of wave vector. The full lines in Fig. 9 are the results of calculations based on the theory by Elliot et al.

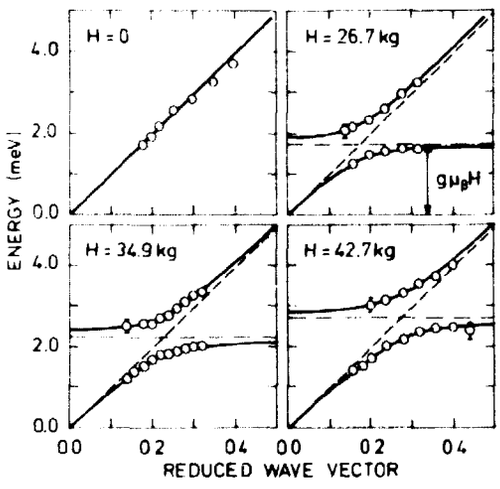

Fig. 9. Observed (o) and calculated (——) energies for the coupled acoustic phonon quadrupole excitation modes in $TmVO_4$ at 4.5 K as function of the reduced wave vector along a <100> direction and for different applied magnetic fields.

27) R. J. Elliot et al., Proc. Roy. Soc. A328, 217 (1972).

28) J. K. Kjems, W. Hayes, and S. H. Smith, Phys. Rev. Lett. 35, 1089 (1975).

using the coupling parameters that were obtained from the temperature dependence of the corresponding elastic constant (c_{44}) in zero field. The excellent agreement shows that the Debye picture can be used for the strain field produced by an acoustic phonon at finite wave vectors in the region where the dispersion is linear.

1.19 Magnetic Excitations and Critical Scattering in Pr_3Tl

(J. Als-Nielsen, J. K. Kjems, R. J. Birgeneau, (Massachusetts Institute of Technology, U.S.A), and W. J. L. Buyers, (Chalk River, Canada))

The detailed mechanism for the onset of magnetic ordering in singlet-ground-state systems, such as Pr_3Tl, has not yet been established. The simplest theoretical picture (random phase approximation), which involves the complete softening of the singlet-triplet transition (Γ_1-Γ_4) in this material, did not agree with an earlier neutron experiment [29]. Since then, more general approaches have been suggested by several authors [30], and the qualitative new feature of these models is the divergence at the transition temperature T_c of the elastic response, originating in transitions with diagonal matrix elements with the excited states. Such a response has now been observed in a high-resolution, small-angle neutron scattering study of a polycrystalline sample of Pr_3Tl. The observed profiles are typical of critical magnetic scattering with a divergence at $q = 0$ and $T = T_c = 11.6$ K. The energy spectra contains two components, a narrow "quasi-elastic" and a broad "inelastic" feature. Tentatively, the broad feature can be associated with a tetragonal splitting of the first excited state (triplet in cubic symmetry), since the point symmetry at the Pr^{+3} sites is D_{4h} in the ordered alloy. This is consistent with an additional energy broadening of the singlet-triplet transition, that is observed in Pr_3Tl when compared to face-centered cubic Pr.

---

[29] R. J. Birgeneau, J. Als-Nielsen and E. Bucher, Phys. Rev. Lett. 27, 1530 (1971).

[30] W. J. L. Buyers and T. Holden, Phys. Rev. B11, 266 (1975).

1.20 Elastic Magnetic Scattering in Pr Metal

(W. J. L. Buyers (Chalk River, Canada), J. G. Houmann, B. Lebech, A. R. Mackintosh, O. D. McMasters*, and K. A. Gschneidner, Jr.* (*Iowa State University, U.S.A.))

The elastic scattering from a large (670 mm^3) single crystal showed [31] broad but weak peaks symmetrically around the (001) and (003) reciprocal lattice points in the <100> directions (ΓM). These peaks showed structure, and have an overall line width of about five times the full width at half maximum of the nuclear (004) Bragg reflections. The peak intensity decreases nearly linearly with temperature and almost becomes unobservable at about 12 K. The scattering may be evidence of a central mode at $q = 0.25Å^{-1}$, in which case similar intensity is expected at $q = 0.25Å^{-1}$ in the <110> directions (ΓKM). A search for elastic scattering around the (003) reciprocal lattice points in the <110> directions showed a broad peak at $q = 0.25Å^{-1}$. This peak has disappeared at 18 K.

1.21 Critical Neutron Scattering in EuO

(O. W. Dietrich and J. Als-Nielsen)

Neutron scattering measurements below the Curie temperature T_c in EuO and in other ferromagnets have shown that the longitudinal spin fluctuations (fluctuations along the direction of the spontaneous magnetization) do not appear as observable diffusive peaks centered around zero energy transfer, as predicted by theory. The longitudinal response at small wave vectors in ferromagnets is most likely strongly coupled to the transverse response (spin waves) and has a two-peaked spectral form, that reflects the spin wave energy. Vaks et al.[32] have suggested a coupling leading to such a response.

Magnetic neutron scattering measures only the response perpendicular to the scattering vector. Therefore, only the transverse magnetic response is measured when all magnetic domains in the sample align with their spontaneous magnetization parallel to the scattering vector. With random orientation of domains, two-thirds of the transverse plus one third of the longitudinal res-

---

31) B. Lebech, J. G. Houmann, and M. Chapellier, Risø Report No. 320, 18 (1974).

32) V. G. Vaks, et al., Soviet Physics JETP 26, 647 (1968).

ponse would be observed. An attempt was made to use this effect to separate the transverse from the longitudinal response in EuO. A powder sample of ^{153}EuO was placed in a 2.4 kOe conventional magnet and the energy spectra of the scattered neutrons were measured in the vicinity of T_c, both with and without the magnetic field along the scattering vector. The effect of applying the field was spectacular (Fig. 10), but unfortunately the results could not be interpreted for the following reason. When applying

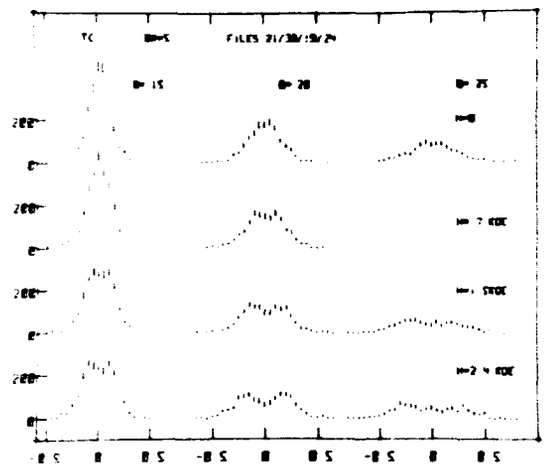

Fig. 10. Energy spectra of critical magnetic scattering in EuO at T_c for various wave vectors (Q) and magnetic fields (H). In zero field the spin dynamics are purely diffusive, as evidenced by a single peak in the scattered neutron spectra. However, even in moderate external magnetic fields, the spin dynamics become propagative, displaying two characteristic spin wave peaks. NB: This figure is an example of the scope of the new data-handling system available at the Physics Department. The raw data are stored on magnetic cassette tape, and processing and plotting are performed by the Hewlett-Packard HP-9830A computer.

a field to a magnetic substance, the domains start aligning along the field direction. This in turn creates a demagnetization field from the "surface poles" formed as a result of the alignment, which will counteract the external field to retain the state of zero internal field as long as possible. Only when all domains are aligned will the external field penetrate to the interior of the sample. Obviously, our intention was to use an external magnetic field equalling the maximum demagnetization field, because then all domains would be aligned but the internal field would still

vanish. A vanishing internal field is a necessary condition for the separation of the transverse and longitudinal responses; otherwise the spin dynamics would not be the same with and without the external field. However, the powder sample did not have a well-defined demagnetization field, probably because of varying shapes of the crystalline grains. Hence, even when applying external fields too small to align the domains, we observed a significant change of the spin dynamics itself. This problem could be circumvented by using a single crystal of ^{153}EuO of ellipsoidal shape. We hope that it will be possible in the future to perform this experiment and thus directly to observe the hitherto obscure longitudinal spectral shape function in a ferromagnet.

1.22 Critical Fluctuations in the Dipolar-coupled Ising Ferromagnet $LiTbF_4$

(J. Als-Nielsen and I. Laursen (The Technical University of Denmark))

The pronounced anisotropic q-dependence of the critical scattering from a dipolar-coupled Ising ferromagnet necessitates a resolution of the order of 0.001 $Å^{-1}$ along the Ising axis. In order to resolve the correlation range 1% above T_c, the q-resolution per-

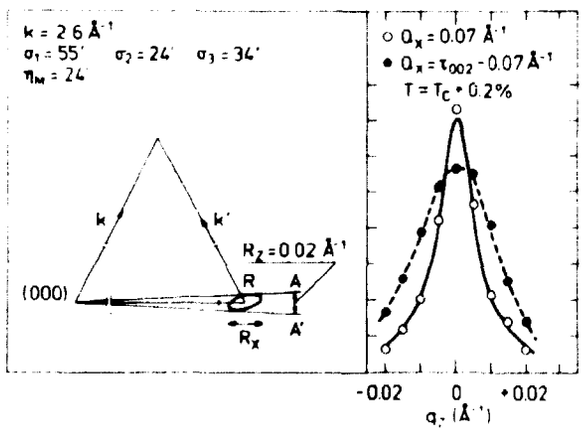

Fig. 11. The extremely narrow resolution that can be obtained in forward elastic scattering, in the direction perpendicular to the scattering vector, is illustrated by results obtained for $LiTbF_4$ of a scan near a reciprocal lattice point and at the equivalent position in forward scattering.

pendicular to the Ising axis should be of the order of 0.01 $Å^{-1}$. These requirements can be met by using small angle scattering techniques and cold neutrons, respectively. The 1/v absorption cross section of ^{6}Li then becomes prohibitive, but this difficulty was overcome by growing a $^{7}LiTbF_4$ crystal. Figure 11 shows results that illustrate the narrow resolution obtained in the forward direction. The results for $LiTbF_4$ are in remarkable agreement with the pioneering theoretical work by Larkin and Khemel'mitskii [33], and also with the results of renormalization group analysis. In particular, our data are supported by the findings of Aharony and Halperin [34], who derived a universal relation between the magnitude of the correlation range and the specific heat.

1.23 Critical Fluctuations in a Two-Dimensional, Site-Random Antiferromagnet $Rb_2(Mn_{0.5}Ni_{0.5})F_4$

(J. Als-Nielsen, R. J. Birgeneau (Massachusetts Institute of Technology, U.S.A.), and G. Shirane (Brookhaven National Laboratory, U.S.A.))

A neutron scattering study of the order parameter, correlation length and staggered susceptibility of the two-dimensional random

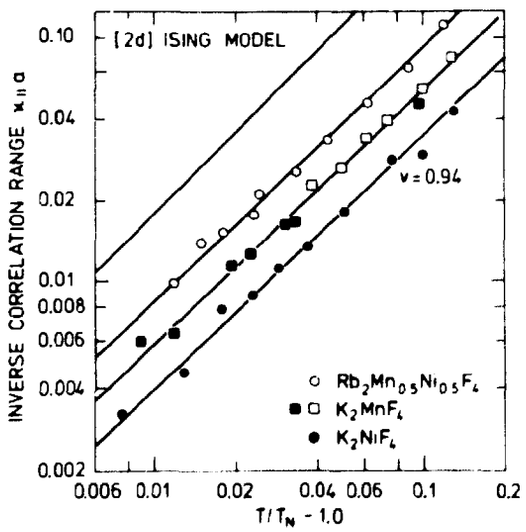

Fig. 12. Longitudinal correlation range near the critical point in the pure materials K_2NiF_4 and K_2MnF_4 and in the random alloy $Rb_2(Mn_{0.5}Ni_{0.5})F_4$. For all three materials the critical exponent ν is close to that of the [2d]-Ising model, whereas the absolute value of N decreases with decreasing anisotropy as given by the ratio of the anisotropy field to the exchange field. This ratio is 0.7%, 0.4%, and 0.2% for $Rb_2(Mn_{0.5}Ni_{0.5})F_4$, K_2MnF_4 and K_2NiF_4, respectively.

---

[33] A. I. Larkin and D E. Khemel'mitskii, Zh. Eksp. Teor, Fiz. 56, 2087 (1969).

[34] A. Aharony and B. I. Halperin, Phys. Rev. Lett. 35, 1308 (1975).

antiferromagnet $Rb_2(Mn_{0.5}Ni_{0.5})F_4$ was carried out partly at Risø, partly at Brookhaven, and the critical behaviour was compared to that of the isomorphous pure materials K_2NiF_4 and K_2MnF_4 (Fig. 12). In these weakly anisotropic materials separation of the diverging longitudinal susceptibility from the finite but large transverse susceptibility is essential. In contrast to earlier work on the pure materials, we now find that the critical exponents are quite similar to those of the two-dimensional Ising model. The effect of randomness on the critical behaviour may be related to the critical exponent α for the specific heat using an heuristic argument by Harris [35]: if $\alpha>0$ randomness should imply a significant change in the critical behaviour, but if $\alpha<0$ randomness should be irrelevant. In our case $\alpha=0$ and it therefore represents an interesting boundary case. We find that randomness has no measurable effect on phase transition behaviour.

1.24 Critical Fluctuations in Tb with the Spiral Phase Suppressed by a Magnetic Field

(J. Als-Nielsen and O. Rathmann)

Magnetization measurements have shown that the spiral phase in Tb which exists from 216 to 226 K may be completely eliminated by a modest magnetic field. We expect to see an anomalous q-dependence of the critical scattering at the critical magnetic field where the spins cannot decide whether to order ferromagnetically or to a spiral structure. Similarly, the dynamic response function should exhibit anomalous behaviour. So far we have obtained a preliminary phase diagram in the (H,T) plane by measuring the Bragg scattering of the $(0,0,2\pm Q)$ satellites at different temperatures (T) and magnetic fields (H).

1.25 Soft-Mode Studies in Chloranil

(W. D. Ellenson and J. K. Kjems)

From nuclear quadrupole, heat capacity, and X-ray measurements[36], the molecular crystal chloranil (2, 3, 4, 5, tetra-chlorobenzo-

---

35) A. B. Harris, J. Phys. C: Solid State Phys. 7, 1671 (1974).

36) H. Terauchi et al., J. Chem. Phys. 62, 3832 (1975) and references therein.

quinone) was found to undergo a second-order phase transition at 92 K. The upper phase is monoclinic naphthalene-like (C_{2h}^5) with two molecules per unit cell. The phase transition involves the condensation of a $\bar{q} = (0,0,\pi/c)$ librational mode leading to a doubling of the unit cell along the c-axis and, as the temperature is lowered, an increasing amount of static rotation about the molecular axis. The order parameter in the low temperature phase is related to the degree of static rotation and was determined from the Bragg intensities of reflections at (m,0,n, + ½) (m and n integers) lattice points in the high temperature cell. The soft mode and the dispersion of the soft mode were successfully observed in the initial neutron scattering. Among the noteworthy features of these spectra are the well-defined phonon groups at room temperature and the fact that these groups merge into an unresolved central peak structure as the temperature approaches the transition point. Current investigations concentrate on measurements of the change of energy of these phonons with temperature and on a study of the line shapes and possible critical scattering near the transition point. These results will be compared to the soft-mode behaviour seen in many other systems, for example, the perovskite $SrTiO_3$.

1.26 Neutron Scattering Studies on CsDA and DCsDA

(G. M. Meyer and O. W. Dietrich)

The ferroelectric properties of CsDA (CsH_2AsO_4) and DCsDA (CsD_2AsO_4) are in many ways similar to those of KDP (KH_2PO_4) and DKDP (KD_2PO_4). There have, however, been several reports that the transitions in the former materials may be more complex than in the latter [37-39]. Neutron scattering measurements were therefore made on CsDA and DCsDA in the hope of elucidating this behaviour. The satellite peaks previously observed [37] between Bragg reflections in the ferroelectric phase were found to arise not from a complex crystallographic structure, but from multiple Bragg scattering processes in which the two scat-

---

[37] O. W. Dietrich, R. A. Cowley, and S. M. Shapiro. J. Phys. C: Solid State Phys., 7, L239 (1974).

[38] N. Lagakos and H. Z. Cummins. Phys. Rev. Lett. 34, 883 (1975).

[39] R. J. Pollina and C. W. Garland, Phys. Rev. B12, 362 (1975).

terings occur in different ferroelectric domains. Another phenomenon studied is the existence of the Bragg scattering associated with the paraelectric phase far below the transition to the ferroelectric phase in DCsDA. The origin of this scattering appears to be inhomogeneities caused by insufficient deuteration of the DCsDA samples used in experiments. We also measured the temperature variation of the orthorhombic shear angle and the elastic constant c_{66}. The latter is much smaller than c_{66} in KDP and this explains the larger temperature difference found between the free and clamped Curie temperatures for CsDA[38].

1.27 High Pressure Structural Transitions in C_6D_6 and $C_{10}D_8$

(B. Buras and W. D. Ellenson)

A neutron diffraction study at high pressure of several closely related molecular crystals was initiated in order to determine the high-pressure structures of these materials. Benzene, C_6D_6, has one structural phase transition at ∿12 kbar and 300 K and one at ∿30 kbar and ∿670 K [40]. The first of these transitions was previously studied both by X-ray techniques [41] and by light scattering [42]. These studies indicated a transition to a structure similar to that found in naphthalene ($C_{10}D_8$) at atmospheric pressure and 300 K. $C_{10}D_8$ has a transition at ∿30 kbar and 543 K to a yet unknown structure. Recently, however, it was shown that $C_{10}F_8$ [43] (at 0 kbar, ∿250 K) undergoes a transition which does not change the space group but only changes the relative molecular packing arrangement. It is possible that the high-pressure transition of $C_{10}D_8$ is of the same type.

---

40) S. Block et al., Science 165, 586 (1970) and references therein.

41) G. J. Piermatini et al., Science, 165, 1250 (1969).

42) W. D. Ellenson and M. Nicol, J. Chem. Phys. Phys. 61, 1380 (1974).

43) G. W. Pawley and O. W. Dietrich, J. Phys. C: Solid State Phys. 8, 2543 (1975).

44) B. Buras, B. Lebech, W. Kofoed, and G. Bäckström, Risø Report No. 300, 44 (1973).

The present diffraction studies of C_6D_6 and $C_{10}D_8$ at pressures from 0 and ∿30 kbar and of temperatures from 300 to 600 K were made possible by a modification of a previously described pressure cell [44]. In C_6D_6 we observed the transition at ∿12 kbar and 300 K. The positions and intensities of the powder diffraction pattern agreed with the previously assigned naphthalene-like structure. The study of the transition in $C_{10}D_8$ is experimentally more difficult since the transition occurs close to pressure and temperature limits of the high pressure cell. We have thus not yet succeeded in observing the phase transition. The diffraction patterns obtained allow an estimate of the anisotropic isothermal compression.

1.28 The Solid to Liquid Phase Transition

(J. Klæstrup Kristensen (The Technical University of Denmark) and R. M. J. Cotterill))

Neutron scattering experiments were performed on Al and Pb in order to investigate the melting transition on an atomic level. From the dislocation theory of melting, according to which melting occurs when dislocations are spontaneously created, one could expect an accompanying softening of the phonons. Although computer experiments have revealed the spontaneous creation of Shockley-type dislocations in fcc crystals, neutron scattering experiments did not show any sign of softening of the associated (111) transverse phonon even as near to the melting temperature as $1/10^{o}C$.

Considered together with the fact that many experiments of the thermodynamic type do show pre-melting phenomena, this has led to a new theory for the melting transition which also bridges the gap between the atomistic dislocation model and the thermodynamic approach. In this theory melting is regarded as starting from the surface without activation energy, and melting occurs, as predicted also by the dislocation theory, at the temperature at which a crystal with the highest possible dislocation density has the same free energy as a perfect crystal. It is important to distinguish between the thermodynamic melting temperature and the crystal instability temperature, at which dislocations are

spontaneously created in the bulk crystal (as seen in computer experiments). The reason why superheating of real crystals is normally not observed is that, at a free surface, dislocation loops can be generated without activation energy once the thermodynamic melting temperature has been reached. The free surface thereby acts as a nucleus for melting. Grain boundaries can also act as a nucleus for melting, and this explains the greatly enhanced grain growth rate that has been observed in polycrystals near T_M.

1.29 Neutron-Scattering Study of Transitions to Convection and Turbulence in a Nematic Liquid

(H. Bjerrum Møller and T. Riste (IFA, Kjeller, Norway))

The intensity of the neutron diffraction peak at 1.8 $Å^{-1}$ of the liquid crystal PAA (para-azoxyanisol) is, in its nemetic phase, a measure of the molecular orientation, which in turn is coupled to the velocity gradient in the liquid. A study of the neutron scattered intensity therefore yields information on the flow properties of liquid PAA in its nemetic phase. When a vertical temperature gradient ΔT is imposed on a liquid, the quiescent state breaks down when ΔT exceeds a critical value of ΔT_c. This phenomenon is usually referred to as the Rayleigh-Benard problem. Heat is transported by conduction for $\Delta T<\Delta T_c$, and by convection for $\Delta T>\Delta T_c$. The convective flow pattern is one of rolls, in which the particles move in two-dimensional orbits of elliptical shape. By further increase of ΔT, the steady-state convective motion becomes unstable and changes to a time-dependent, turbulent motion. Recent theories [45] of the transition to turbulence predict the existence of a regime of time-dependent, periodic motion before fully developed turbulent motion is reached at large gradients.

We have studied the onset of turbulence in nemetic PAA using the technique of neutron diffraction [46]. The transition to turbulence was indeed found to occur through two successive

---

[45] M. B. McLaughlin and P. C. Martin, Phys. Rev. A12, 186 (1975).

[46] H. B. Møller and T. Riste, Phys. Rev. Lett. 34, 996 (1975) and H. B. Møller, T. Riste, Fluctuations, Instabilities and Phase Transitions. Edited by T. Riste (Plenum Press, New York and London) 313 (1975).

instabilities. The first of these clearly signals the entrance to a regime with large periodic fluctuations, and the second, although less clearly, to a regime with non-periodic, time-dependent motion. Experiments were also carried out to observe these phenomena by visual inspection. Here the sample cell was placed between crossed polarisers in transmission geometry in a strong light beam. A rectangular box with a good aspect ratio (length 25 mm, width 7.5 mm and height 2.5 mm) was used. This cell was almost opaque when the liquid was in the nematic phase and quite transparent when the liquid was in the isotropic phase. The development of the convective roll pattern was therefore easily seen in the two-phase system containing about the same amount of liquid in the nematic and in the isotropic phases. This system exists when the average temperature is kept constant at the clearing point. The following qualitative observations were made. At negative gradient (the top of the sample warmer than the bottom), there is a clear horizontal separation between the nematic and isotropic liquid characteristic of the conductive region. At an infinitesimally small positive gradient, a flow pattern consisting of two stationary rolls develops. As the gradient increases, four stationary rolls appear and, at still higher gradients, the flow pattern develops into a time-dependent pattern in which rolls seem to develop all over the cell and die away again.

1.30 Canonical Band Theory of the Volume and Structure Dependence of the Magnetic Moment of Fe

(J. Madsen (The Technical University of Denmark), O. K. Andersen U. K. Poulsen, and O. Jepsen)

The ferromagnetic moment at 0 K of bcc, hcp and fcc Fe was obtained as a function of atomic volume from self-consistent, spin-polarized band calculations employing the linear muffin tin orbital method [47] and the local spin density approximation for exchange-correlation [48,49]. The results (Fig. 13) are in good agreement with the measured bcc moment of Fe and in fair

---

[47] O. K. Andersen, Phys. Rev. B12, 3060 (1975).

[48] U. von Barth and L. Hedin, J. Phys. C: Solid State 5, (1972).

[49] O. Gunnarsson et al., Solid State Commun. 11, 149 (1972).

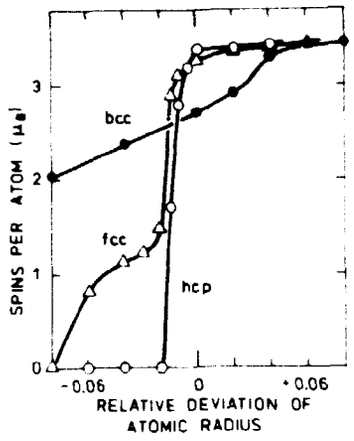

Fig. 13. The ferromagnetic moment of Fe as a function of atomic radius and crystal structure. The sp-d hybridization is neglected.

agreement with the volume dependence of the bcc moment. They show a very strong volume dependence of the hcp and fcc moments near the usual atomic volume, and they explain the pressure induced (bcc, ferromagnetic) to (hcp, paramagnetic) transition around 100 kbar. These findings have a simple interpretation in terms of the Stoner criterion and the bcc, hcp and fcc canonical d-state densities [50]. We are presently computing the isomer-shifts. These calculations would be impossible with conventional techniques since they require several hundred individual band-structure calculations. We have therefore developed a method by which a smaller number of band-structure calculations and the corresponding Brillouin zone integrations may be performed once and for all for a given crystal structure.

1.31 Spin Density of Pd_3Fe

(O. Jepsen and O. K. Andersen)

Self-consistent, spin-polarized band calculations, using the linear muffin tin orbital method [47], are being performed with the aim of computing the magnetic form factors of simple cubic Pd_3Fe from first principles. So far, the paramagnetic energy bands and their state density have been determined.

---

50) O. Jepsen and O. K. Andersen, Risø Report No. 300, 30 (1973) and No. 320, 38 (1974).

1.32 Electronic Structure of Na-W Bronzes

(J. Damgård, O. Jepsen, O. K. Andersen, and A. R. Mackintosh)

There have long been discussions on the conduction mechanism in the Na_xWO_3 compounds [51] that are stable for $0<x<1$. The energy bands of Mattheiss [52] for the stoichiometric compound with $x = 1$ and the perovskite structure indicate that the W 5d-electrons rather than the Na 3s-electrons are responsible for the conduction. However, charge-transfer was not properly treated in the Mattheiss calculation. We are therefore modifying the linear muffin tin orbital computer routines used for the Pd_3Fe-structure in order to calculate the $NaWO_3$-bands self-consistently.

1.33 Electronic Structure and Magnetic Breakdown in Ti

(O. Jepsen)

The electronic energy bands of the three-dimensional, hcp transition metal Ti were calculated by the linear muffin tin orbital method [47] including the non-spherical contribution to the cellular potential and all relativistic effects. The agreement between the calculated Fermi surface and the de Haas-van Alphen measurements [53] is the best so far obtained from first principles for a three-dimensional metal. Magnetic breakdown was found to be important. The good agreement for Ti allowed us to reanalyze the de Haas-van Alphen data of the iso-electronic four-dimensional metal Zr with the results that all measured branches could be associated with the theoretical Fermi surface [54].

---

51) A. R. Mackintosh, J. Chem. Phys. 38, 1991 (1963).

52) L. F. Mattheiss, Phys. Rev. B6, 4718 (1972).

53) G. N. Kamm and J. R. Anderson, Low Temperature Physics-LT13 (Plenum Press, New York) 114, (1974).

54) O. Jepsen, O. K. Andersen, and A. R. Mackintosh, Risø Report No. 320, 40 (1974) and Phys. Rev. B12, 3084 (1974).

1.34 Temperature Dependence of the Lattice Dynamics of ^{7}Li

(M. M. Beg and M. Nielsen)

Phonon dispersion relations in ^{7}Li were determined by coherent inelastic neutron scattering at 293 and 110 K. The frequency distributions were obtained from the experimental data using the Born – von Karman general force model. The first neighbour force constants at 293 K were found to be ∿10% smaller than those at 110 K. At both temperatures the fifth order constants were

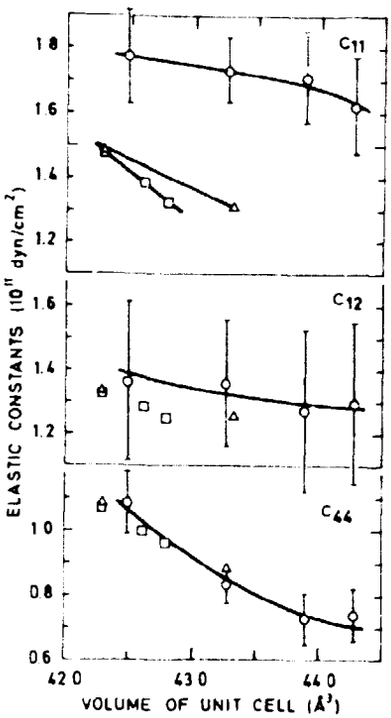

Fig. 14. Volume dependence of the elastic constants determined by neutron diffraction (o) compared to the values determined by the sound echo technique by Nash and Smith[55] (□) and Jain[56] (Δ). The measurements at the largest volume correspond to a temperature of 0.94 of the melting point. The solid lines are for ease of reading.

found to be ∿3% of the first order constants. Therefore five neighbour Born-von Karman fits were adequate. The elastic constants derived from the model parameters at 293 K are in (10^{11} dyn/cm^2) c_{11} = 1.73 ± 0.10, c_{12} = 1.31 ± 0.20 and c_{44} = 0.830 ± 0.060.

The temperature dependence of the low energy and the zone boundary phonons was studied from 110 K to near the melting point. The

---

55) H. C. Nash and C. S. Smith, J. Phys. Chem. Solids, 9, 113 (1959).

56) A. L. Jain, Phys. Rev. 123, 1234 (1961).

temperature dependence of the elastic constants was determined from the initial slope of the dispersion relations. The lattice parameter was found from neutron diffraction to be 2.490 ± 0.003 Å at 110 K and 3.537 ±0.003 Å at 424 K. From these results the volume dependence of the elastic constants shown in Fig. 14 was determined. Also shown on Fig. 14 are the elastic constants determined by the sound echo technique [55,56]. The energy shifts and the widths of the zone boundary phonons were evaluated at 293, 383, and 424 K by comparing the widths and energies to those measured at 110 K. Even near the melting point distinct phonon peaks were observed and their widths were smaller than 20% of the phonon energy.

1.35 Neutron Scattering in C_2F_6

(E. Warming)

The plasticity of a molecular crystal arises from the fact that it is very easy to create and move lattice defects, because of the mobility of the molecules. Therefore it is easy for a large number of dislocations to move through the lattice and change the orientation of the crystal. C_2F_6 has a plastic phase between 104 and 172 K. It is not difficult to grow a crystal of C_2F_6 but because of the placticity the crystal reorient, i.e., it has a limited lifetime. This lifetime decreases with increasing temperature and decreasing mosaic spread. In the plastic phase the structure of C_2F_6 is bcc and the cube edge varies linearly from 6.087 ± 0.002 Å at 104 K to 6.254 ± 0.002 Å at 172 K. Measurements on one of these rather rapidly changing crystals (lifetime about a week and with a mosaic spread of $\sim 0.50^{o}$) revealed some excitations. If these are accepted as phonons they indicate sound velocities in the <110> and <100> directions of 100 - 200 m/s. This corresponds to elastic constants of the order of 10^8 dyn/cm^2, i.e. $\sim 10^2$ times lower than for other solids. From a set of powder diffraction scans a rough estimate of an effective Debye-Waller factor, exp $(-2B \sin^2\theta/\lambda^2)$ gives $B \sim 1.5$ Å^2 at 115 K.

1.36 Structure and Dynamics of Monolayers of H_2 and D_2 Adsorbed on Grapnite

(M. Nielsen and W. D. Ellenson)

The structure and dynamics of H_2 and D_2 molecules adsorbed on grafoil were measured with neutron scattering. Grafoil is a partly-oriented graphite product that acts as a good substratum for thin layers of adsorbed gases. At low temperatures both H_2 and D_2 form a two-dimensional, solid-like monolayer on the graphite surface. This monolayer has a simple triangular structure observable by means of elastic neutron scattering. The position of the (10) Bragg reflection varies with the amount of H_2 or D_2 gas adsorbed, as shown in Fig. 15. At low fillings the reciprocal lattice vector of the (10) reflection equals 1.703 $Å^{-1}$. This lattice vector corresponds to a $\sqrt{3}$-structure having one gas molecule situated above every third carbon hexagon of the graphite surface. The monolayer is compressed into a non-commensurate

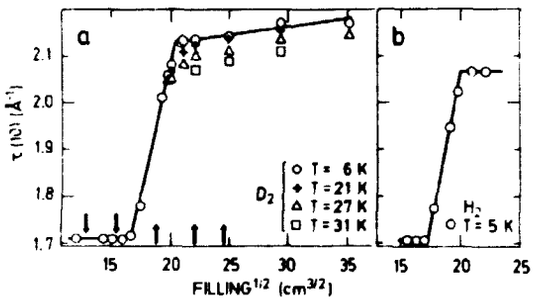

Fig. 15. The position of the diffraction peaks from monolayers of D_2 and H_2 as function of the square root of the amount of gas adsorbed.

triangular structure when more gas than needed to cover the entire graphite surface with the $\sqrt{3}$-structure is added to the sample cell. The spacing between the molecules of the non-commensurate structure varies linearly with the square root of the number of molecules until the densest possible monolayer is reached. At this stage the second layer of adsorbed H_2 or D_2 starts being formed. For both H_2 and D_2, the $\sqrt{3}$-structure melts at 20 K, whereas the densest possible monolayer persists up to $\sim$ 30 K.

The dynamics of the adsorbed monolayers of H_2 and D_2 were studied by inelastic neutron scattering. It was found that the dynamics depends dramatically on the density of the layers. Figure 16a

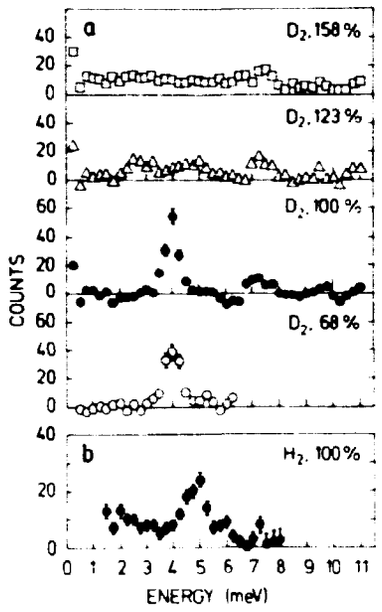

Fig. 16. Coherent neutron scattering groups at 4.2 K from adsorbed monolayers of D_2 (a) and H_2 (b). The amount of gas adsorbed on the grafoil relative to the amount of gas needed to cover the total graphite surface with a monolayer having the $\sqrt{3}$-structure is given on the figure.

shows a coherent one-phonon response for the neutron scattering vector parallel to the layer of a two-dimensional powder of D_2-monolayers. The two lower scans show the scattering from monolayers having the $\sqrt{3}$-structure. A single peak is observed at 4 meV with a full width at half maximum (FWHM) of $\sim$ 0.3 meV. The peak does not change with the scattering vector, and this indicates that the molecules in the $\sqrt{3}$-structure behave like localized oscillators with weak interaction between neighbouring D_2 molecules. However, for the non-commensurate structures, the inelastic neutron scattering response differs. It resembles the broad energy spectrum observed in ordinary three-dimensional solid powders. A similar dynamic behaviour is observed for adsorbed H_2 monolayers. (Fig. 16b). For the $\sqrt{3}$-structure, a single coherent peak is observed at 5 meV with a FWHM of $\sim$ 1 meV.

1.37 Dynamics of H_2 Adsorbed on Al_2O_3

(M. Nielsen, I. Silvera (University of Amsterdam, The Netherlands), and W. D. Ellenson)

Activated Al_2O_3 may be used to prepare enriched samples of ortho-hydrogen and para-deuterium (o-H_2 and p-D_2) that both have odd

rotational quantum numbers [57]. Separation is obtained by preferential adsorption of the J=1 molecules at liquid hydrogen temperatures. We have initiated neutron scattering measurements from H_2 molecules adsorbed on activated Al_2O_3 in order to study the state of the adsorbed p-H_2 and o-H_2 molecules. The intensity was measured of the conversion scattering where a neutron scatters a para-molecule into the ortho-state. For freely rotating

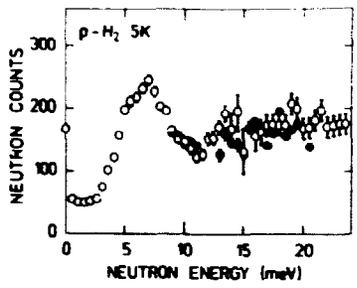

Fig. 17. Neutron scattering at 5 K from p-H_2 molecules adsorbed on activated Al_2O_3. The data were obtained with about 740 cm³ of H_2 gas adsorbed on 45 g Al_2O_3.

molecules this gives a strong scattering at the energy transfer 14.6 meV, which equals the rotational energy of the J=1 molecules. This is observed both in the scattering from solid H_2 and from H_2 molecules adsorbed on graphite. For H_2 adsorbed on Al_2O_3 we observed a spectrum with a broad peak at 5-7 meV (Fig. 17). This indicates that although the ortho-para properties of the adsorbed molecules are preserved, the rotational energy of the ortho-molecules is partly quenched in the adsorbed phase.

1.38 Mosaic Structure of Single-Crystals Studied by γ-Ray Diffraction

(Knud Møllenbach)

A γ-ray diffractometer, similar to that described by Schneider[58], was built (Fig. 19) and tested. γ-radiation of an energy of 412 keV and with an angular divergence of 10" is obtained from an activated Au-foil (125 Ci ^{198}Au) using single-slit beam-definers of lead. After diffraction in a sample the scattered radiation is detected by means of scintillation counter. A goniometer

57) D. A. Depatie and R. L. Mills, Rev. Sci. Inst. 39, 105 (1968).
58) J. R. Schneider, J. Appl. Cryst. 7, 541 (1974).

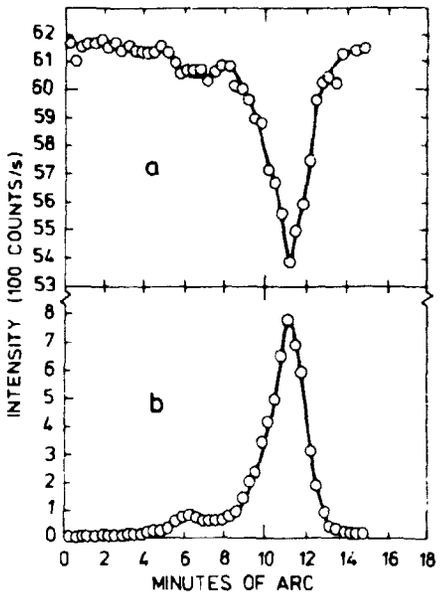

Fig. 18. Rocking curve of a pressed Ge crystal measured at the γ-ray diffractometer.
a) Transmitted primary beam.
b) Diffracted beam. Note that the sum of the intensities is constant over the angular range investigated. This indicates that the measured scattering is free of multiple scattering.

system makes it possible to rotate the sample about one vertical and two horizontal axes. The vertical rotation is very precise (down to steps of 2") and this makes the instrument a useful tool for studying the mosaic structure of single crystals. An example of a rocking curve measured by the γ-ray spectrometer is shown in Fig. 18.

The performance of the instrument is investigated by comparing experimental data (resolution and reflectivity with analytical calculations and computer simulation (Monte Carlo technique)[59].

---

59) K. Møllenbach, Master's Thesis, The Technical University of Denmark (1975).

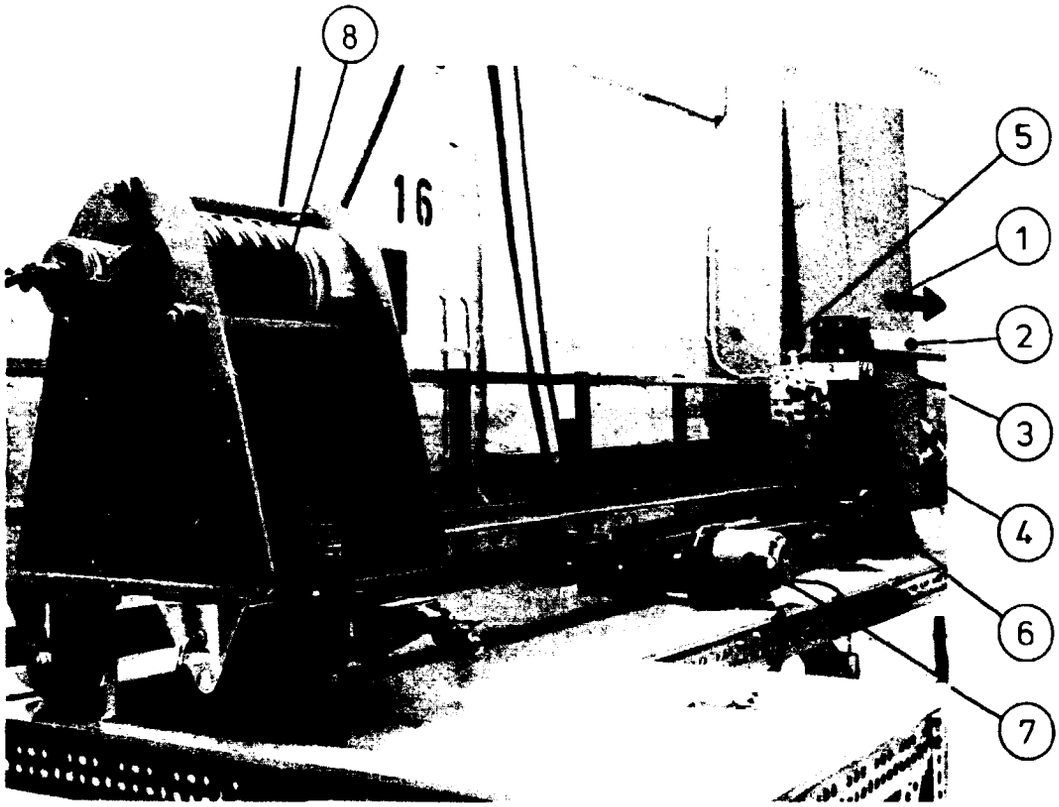

Fig. 19. The γ-ray diffractometer. 1) Direction to the γ^- source. 2) Guide tube 50 mm in diameter. 3) Variable slit defining the beam. 4) Goniometer system. 5) Sample. 6) Handle for coarse sample rotation. 7) Step motor for fine sample rotation. 8) Scintillation counter.

2. PLASMA PHYSICS

The plasma physics section works under a contract of association between the Danish Atomic Energy Commission and Euratom. The activities are centered on technology of interest for future fusion reactors (2.1-2.6) and on basic plasma physics (2.7-2.12).

The technological aspects of plasma physics are undertaken with one of the possible refuelling schemes for fusion reactors in mind. This scheme requires an acceleration technique able to accelerate small pellets to a velocity of the order of 10^3-10^4 m/s. The necessary velocity depends on the ablation rate of a pellet inside a fusion plasma. Studies of interactions between plasmas and solids are therefore of interest. Two basically different approaches are adopted. One (2.1-2.2) is a study of the interactions of a controlled beam of charged particles with films of light elements. The other (2.3-2.6) is an investigation of the interactions of a hot rotating plasma (produced in a puffatron) with solid pellets of light elements.

The main object of the basic research in plasma physics (2.7-2.12) is investigations of waves and instabilities in a relatively cold steady state plasma (produced in a Q-machine). The observation that unstable ion cyclotron waves occur when an ion beam penetrates such a plasma may be of technological interest for heating of a fusion plasma.

2.1 Secondary Electrons From Solid H_2 and D_2

(H. Sørensen)

Work on films of solid H_2 and D_2[60] resulted in a method for determining the secondary electron emission (see) coefficient for ion bombardment. The method utilizes the fact that a film charges up electrically by bombardment with positive ions and then retains the secondary electrons. The initial current collected by the target is $i_+ = i_b(1+\delta_+)$, where i_b is the beam current and δ_+ the see-coefficient. i_+ quickly approaches a saturation value, i_b. When a grid is placed in front of the target a similar method can be used for electron irradiation. If the grid is held at

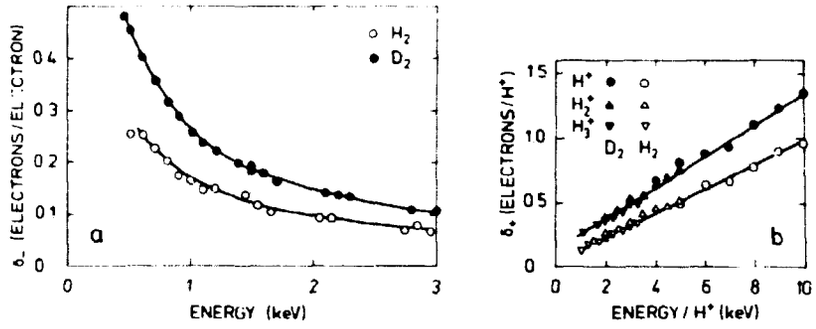

Fig. 20. Secondary electron emission coefficient for normal incidence on solid H_2 and D_2 films. a) Bombardment with electrons; the see-coefficient is defined as emitted electrons per incident electron. b) Bombardment with H^+, H_2^+, and H_3^+-ions; the see-coefficient is defined as emitted electrons per incident H^+-ions.

-45 V with respect to the target, the secondary electrons are retained and the current collected initially equals i_b. The film surface then charges up and an intermediate state is reached in which the secondary electrons can escape. In this state the collected current is $i_- = i_b\ (1-\delta_-)$.

The method was further developed to allow measurements with short beam pulses of ions or electrons (0.3 ms and 10-100 nA) in which case charge-up does not occur. The measurements are thus made on an electrically neutral film. With the grid at -45 V the secondary electrons are retained and the current equals i_b. With the grid at +45 V the secondary electrons are drawn away from the target and the current is i_+ for ion irradiation and i_- for electron irradiation. It was verified experimentally that the charge-up method and the single pulse method agree for small angles of incidence. Measurements of the see-coefficients were made with electrons (0.5 - 3 keV) or H^+, H_2^+, and H_3^+-ions (4-10 keV) incident on D_2 and H_2. The results for normal incidence are shown in Fig. 20 where δ_+, defined as electrons per H^+- ion, is plotted versus energy per H^+- ion. We see that a molecular ion, such as H_3^+, corresponds to three H^+-ions with respect to electron emission.

There is a considerable difference between H_2 and D_2 for both electrons and for ions. The origin of this difference is not yet understood, but if the secondary electrons have different range or lifetime in the two materials the see-coefficients would differ. It may be possible for a secondary electron to lose energy by exciting rotational and vibrational states of the molecules. If such a mechanism has any significance it may explain the observed experimental results. The see-coefficient was also studied for oblique incidence at angles up to 75^{o}. The results obtained at the largest angles may be dubious since back-scattered particles might have influenced the measurements. The angular dependence can be approximately described by $\delta_{\pm}(\theta)=\delta_{\pm}(0)/\cos\theta^{n}$, where n = 3/2 for electrons and n = 5/4 for H-ions.

2.2 Reflection of Energy from Solid Targets Bombarded with keV Protons

(H. Sørensen)

When a beam of fast atomic particles hits a solid surface a fraction of the particle energy is reflected from the surface. The reflected energy shows up as sputtered, desorbed, and back-scattered particles. It was found possible to utilize the set-up[60] built for the study of solid D_2-films to measure the fractional reflected particle energy, γ. γ is determined by calorimetry and the target system acts as a calorimeter where the target surface material can be rapidly changed. When the target is covered with a D_2-film all the particle energy is adsorbed and the beam power, P, may be determined. The film is then removed by slightly heating the target and the adsorbed power is $P(1-\gamma)$. The measurements were made on Au since γ is largest for materials with high atomic numbers. The ions used were H^+, H_2^+, and H_3^+ with energies from 4 to 8 keV. The data obtained agreed well with the measurements[61] made at higher energies at the Niels Bohr Institute and at Aarhus University.

---

[60] H. Sørensen, Risø Report No. 320, 46 (1974).

[61] H. H. Andersen, T. Lenskjær, G. Sidenius, and H. Sørensen. The Energy Reflected from Solid Tangets Bombarded with keV Protons and Helium Ions. J. Appl. Phys. (1976).

2.3 Theory of Refuelling Pellet

(C. T. Chang)

A model describing the interaction between a magnetized plasma and a refuelling pellet was formulated and used to calculate the effect of magnetic shielding on the ablation rate. In view of the possible occurrence of turbulence around an ablating pellet, we examined the influence of turbulence on the energy transport and on the ablation rate of the pellet. Attempts were made to describe the equilibrium potential of a pellet in a fusion plasma environment in terms of, for instance, secondary emission coefficients.

2.4 Electron Temperature Measurements by Laser Scattering

(P. Nielsen)

Previous attempts to measure the electron temperature in the puffatron failed because the laser used was operated at too low an energy. The oscillator-amplifier ruby laser system is presently being modified in an attempt to achieve sufficient energy per laser pulse.

2.5 Pellet-Rotating Plasma Spectroscopy

(L. W. Jørgensen, A. H. Sillesen, and F. Øster)

The velocity of the ablated material from a pellet may be determined [62] by analyzing the light emitted from the tail of the pellet during interaction with H or He plasmas. From measurements of the H_β-light at various distances from the pellet we found that the drift velocity of the ablated (excited) neutrals is about $1\text{-}2\times10^4$ m/s corresponding to 0.5-2 eV. This value seems to be quite independent of the type of plasma and of the plasma energy flux. The drift velocity of the neutrals in the tail behind the pellet and in the domain close to the pellet is almost identical. This is in accordance with a theoretical model [63]

---

62) D. Dimock, M. Platisa, M. Popovic, A. H. Sillesen, and F. Øster, Risø Report No. 320, 66 (1974).

63) L. W. Jørgensen, Risø-M-1923 (1975).

predicting that the velocity of the ablated material should be independent of the energy flux that penetrates to the surface of the pellet.

2.6 Rotating Plasma Characteristics Determined by Measurements of Charge Exchange Neutrals and Doppler Broadening

(L. W. Jørgensen and A. H. Sillesen)

Several energy spectra of charge exchange neutrals were previously obtained[64] by using an uncalibrated neutral particle detector (NDP). This detector has now been calibrated in the energy range 0.5-5 keV at Culham Laboratory. The detector sensitivity versus the neutral particle energy corresponds to similar results obtained elsewhere. By using this energy calibration, we found acceptable agreement between the measured and calculated charge exchange neutral spectra. With the neutral particle detector installed in the mid-plane of the puffatron we

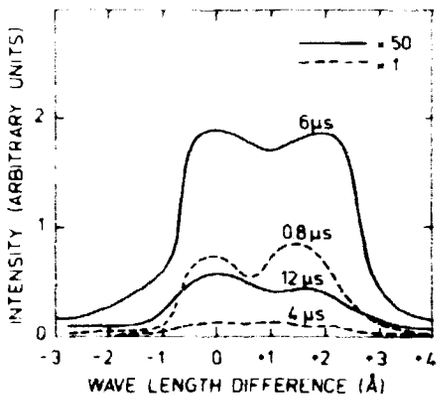

Fig. 21. The Doppler broadening profile development after the start of the discharge. $\Delta\lambda$ = 0 Å corresponds to the cold He_{II}-line (4686Å). The puffatron parameters are: Filling Pressure 0.9 atm, voltage: 25 kV, magnetic field: 1.5 T.

measured the amplitude and time-delay of the detector signal for different positions of the puff-valve. These results give a measure of the delay of the ionization at different positions from the mid-plane and indicate an ionization velocity parallel to the magnetic field of 2×10^4 m/s, which agrees with our earlier results using the diamagnetic loop.

---

64) L. W. Jørgensen and A. H. Sillesen, Risø Report No. 320, 64 (1974).

In helium discharges the Doppler broadening spectra of He_{II} (4686Å) were measured along a chord perpendicular to the magnetic field. The reproducibility from shot to shot was reasonably good and allowed the determination of the ion line profile using a monochromater with a single detector channel. Spectra measured in the direction of the plasma rotation and in the opposite direction were symmetric with respect to the cold He_{II} line, as expected. The results obtained by measuring the Doppler broadening agree well with the ion distribution in hydrogen discharges measured by means of the neutral particle detector. The Doppler broadened line profile indicates that ions preserve their velocities after the breakdown period has ended. Figure 21 shows the development of the He_{II} line profile for a fixed set of puffatron parameters.

2.7 Ion Acoustic Waves Propagating along a Density Gradient

(N. D'Angelo, P. Michelsen, and H. L. Pécseli)

A density gradient along the direction of the magnetic field lines was produced by surrounding a portion of the Q-machine plasma column by a brass tube. The steepness of this gradient could be varied by changing the tube bias, the more negative voltages giving rise to steeper density profiles. The ion acoustic waves propagating along the gradient were examined. At low frequencies we found a relative wave growth, the hydrodynamic growth, which can be predicted from the fluid equations. At higher frequencies, the collisionless wave damping was found to be identical to that of uniform plasmas. The transition frequency at which the wave changes from growth to damping agreed well with calculations made for a plasma in which the density gradient was produced by a gravity field as is the case in the solar corona. When the density gradient was very steep, we observed the generation of higher harmonics of the waves.

2.8 Observation of Ion-Beam-Excited Electrostatic Ion Cyclotron Waves (eicw)

(P. Michelsen, H. L. Pécseli, J. Juul Rasmussen, and N. Sato (Tohoku University, Japan))

An ion beam propagating along the plasma column in the Q-machine was produced in two different ways. In the first method the ion beam was produced by emission from a positively biased ion emitter. The emitter is a filament covered by waterglass (Na_2O, $2SiO_2$) that emits Na-ions when heated to about 1100 K. In the other method, the Q-machine was used as a double-plasma device, i.e., the plasma is produced on two separate hot plates and the plasma column is divided into two parts by a negatively biased grid. When one of the hot plates is positively biased, the ions from this part of the plasma column (the driver plasma) flow into the other part (the target plasma) and produce an ion beam.

When an ion beam was present and other conditions such as high electron temperature and correct beam-plasma density ratio were satisfied, electrostatic ion cyclotron waves appeared. It is well known that these waves can be excited with an electron beam, but only one earlier experiment[65] has indicated the possibility of ion beam excitation. The dispersion relation and the threshold beam energy were measured and found in good agreement with calculations based on a kinetic theory. It was found that the waves propagated along the magnetic field in contrast to previous measurements of waves excited by an electron beam where no propagating waves were found.

2.9 Stability Limits of the Ion-Beam-Excited Electrostatic Ion Cyclotron Instability

(P. Michelsen)

The dispersion relation for low frequency electrostatic waves was analyzed to find the region of stability for an ion beam plasma versus beam velocity v_b and versus the ratio of electron to ion temperature. For low beam velocities it was found that the ion acoustic mode propagating along the magnetic field (k_x=0) was

---

65) H. Ishizuka et al., J. Phys. Soc. Japan 36, 1158 (1974).

unstable at the lowest temperature ratio. When the beam velocity is higher than 1.6 times the ion thermal velocity, the marginal unstable mode propagates at a finite angle to the magnetic field. At even higher beam velocities the plasma becomes unstable at a temperature ratio ~1, and the unstable mode propagates nearly perpendicular to the magnetic field as an electrostatic ion cyclotron wave.

2.10 Ion Acoustic Waves in the Presence of High-Frequency Electron Oscillations

(H. L. Pécseli)

The propagation of ion acoustic waves in collision-free plasmas was investigated using the assumption of Boltzmann-distributed electrons. The influence of short-wavelength, high-frequency electron oscillations was considered, the high-frequency oscillations being treated as wave packets with a distribution in k-space that satisfies the wave kinetic equation. The motion of the wave packets was then studied in a medium slowly varying in space and time, the variation being caused by the low-frequency, long-wavelength, ion acoustic wave. It was demonstrated that high-frequency oscillations may stabilize an initially unstable double-humped ion distribution. The analysis allows generalization to several other low-frequency, long-wavelength, unstable oscillations.

2.11 Electromagnetic Radiation Originating from Unstable Electron Oscillations

(H. L. Pécseli and J. Juul Rasmussen)

The experiment was carried out in a discharge tube where the plasma was created by ionization of an Ar-gas by a fast electron beam. The electron velocity distribution consisted of two components: uncolliding fast electrons and a group of electrons in thermal equilibrium produced by the ionization. For a sufficiently high beam velocity, the electron distribution becomes unstable. Under this condition electromagnetic oscillations in the frequency range 300-700 MHz were detected outside the plasma on a half-wave

dipole antenna. The electromagnetic oscillations were polarized parallel to the discharge axis. In all cases investigated, the radiation pattern was symmetric with respect to a plane perpendicular to the discharge axis. We interpret the radiation as being caused by standing (m=0) electron surface oscillations spontaneously excited because of the unstable electron distribution. Only waves travelling in the direction of the beam are unstable. Reflections at the steep density profiles at the ends of the plasma column give rise to a standing wave (or rather a standing component). Seen from the far-field, a standing wave of N wavelengths may be viewed as an array of N oscillating dipoles orientated along the axis, and it will radiate accordingly although slow surface waves are non-radiating.

2.12 Propagation Properties of Density Pulses in an Ion-Beam Plasma

(P. Michelsen, J. Juul Rasmussen, and N. Sato (Tohuku University, Japan)

The effects of an ion beam traversing a plasma are of current importance in connection with plasma instability and heating, and have received increasing attention in recent years. A convenient experimental method of classifying the ion-beam plasma system as stable or unstable is to observe the behaviour of an excited pulse. Therefore, to emphasize the general features, numerical calculations were made of the propagation properties of density pulses through an ion-beam plasma system, in stable as well as unstable situations, both for pure velocity and pure density modulation. The calculations were based on the linearized Vlasov equation, which was solved with the pertubation as an initial value, using the theory applied by Jensen et al.[66]. The propagation properties were found to be strongly dependent on the chosen modulation. In the case of velocity modulation, a fast positive pulse showed initial growth even under stable conditions and reached a maximum amplitude. However, in the unstable situation the slow pulse interacted with the plasma mode and formed the unstable mode which continued to grow. The

---

66) V. O. Jensen, P. Michelsen, and H. C. S. Hsuan, Phys. Fluids 17, 2203 (1974).

unstable mode consists of a negative and a somewhat slower and smaller positive contribution. In the case of density modulation, growth only appeared in the unstable situation. The unstable mode was similar to that obtained for velocity modulation but the polarity altered.

3. NUCLEAR SPECTROSCOPY

3.1 An Attempt to Form the ^{236}U Fission Isomer with Thermal Neutrons

(V. Andersen, C. J. Christensen, S. Bjørnholm*, J. Borggreen*, and N. J. S. Hansen*(*Niels Bohr Institute, Copenhagen))

The experiment[67] investigating the formation of the fission isomer of ^{236}U by thermal neutron irradiation of ^{235}U was completed. A search was made for coincidences between conversion electrons and L-X-rays from ^{236}U in delayed coincidence with fission fragments. We looked for the fission isomers (half-life $\sim$ 100 ns) in time spectra, using the time difference between conversion electrons and fission fragments. Such a spectrum shows a prompt peak for events with simultaneous conversion electrons, X-rays and fission fragments, and a background contribution from events with simultaneous electrons and X-rays from one nucleus, but in random coincidence with a fission fragment from another nucleus. Superimposed on these events, the isomeric events will show up as a tail to the prompt peak, corresponding to delayed fission fragments with a half-life of 110 ns. Figure 22 shows such time spectra outside the prompt peak for different X-ray energy windows. The spectra show a significant tail when the X-ray window includes the L_α-, L_β-, or the L_γ-peak from the characteristic ^{235}U-L-X-rays, whereas no tail is seen when the X-ray windows are outside the U-L-X-rays. The absence of a tail for X-ray energies outside the U-L-X-rays excludes an instrumental origin of the tails present inside the U-L-X-ray windows. The total number of isomeric events with electron energies from 10 to 1000 keV corresponds to a ratio of isomeric fission to prompt fission of $(9.8 \pm 3.2)10^{-6}$, which is a factor of two below the previously found upper limit[68]. An extensive analysis of the data was made to look for characteristic electron lines corresponding to the transitions in the second well of the fission barrier, but no convincing lines were found.

---

[67] V. Andersen and C. J. Christensen, Risø Report No. 300, 53 (1973).

[68] L. A. Popeko et al., Sov. J. Nucl. Phys. 17(2) 121, (1973).

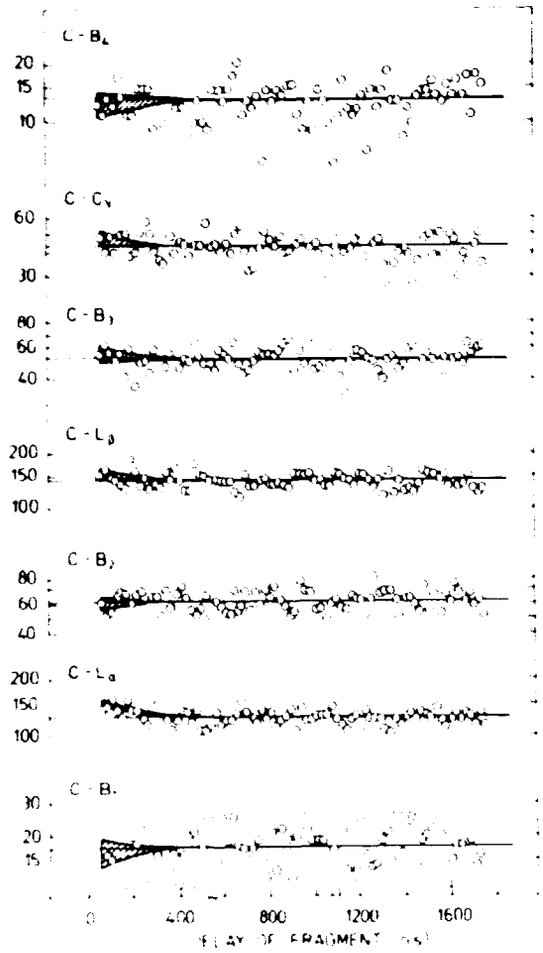

Fig. 22. Electron - fission fragment time spectra for different X-ray energies. The prompt coincidence peaks are omitted. The constant, accidental background is shown as thin lines, whereas the heavy lines show the fitted sum of a constant background and a 100 ns exponential tail as obtained from a least square fit. The two heavy lines in each spectrum correspond to the upper and lower limits of the tail as obtained from the fitting procedure. The X-ray windows B_1-B_2 correspond to X-rays in the energy region of, but not including any of the U-L-X-ray peaks.

3.2 Fine Structure in the Mass Distribution for Fission Fragments

(V. Andersen and C. J. Christensen)

The spectra of mass yields from spontaneous fission and thermal-neutron-induced fission of even nuclei sometimes show a fine structure indicating a preference for doubly even mass division. For a given nucleus, the fine structure is more pronounced when the total kinetic energy carried away by the fragments is larger

than average. This preference for doubly even mass divisions can be interpreted as the preservation of superfluidity during the descent from saddle to scission. Even though it is conceivable that total kinetic energy means low excitation energy of the fragments, and therefore a better chance to avoid breaking of pairs, it seems possible that an appreciable fraction of the excitation energy could be stored in the deformation of the fragments. From this point of view, Bjørnholm[69] suggested that the low kinetic energy events could also be followed by enhanced fine structure. To test this idea, we initiated an experiment designed to measure the fine structure as a function of the total kinetic energy. A better mass resolution than that usually obtained by the two-fragment energy method can be obtained by measuring both the energies adsorbed in and the time-of-flight difference between two surface barrier detectors. Figure 23 shows an example of the pre-neutron mass distribution for fission fragments from ^{252}Cf, when large total kinetic energy is carried away by the fragments.

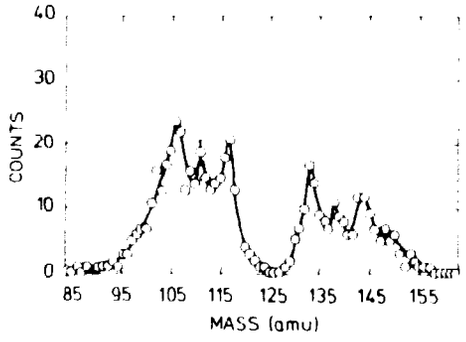

Fig. 23. Pre-neutron mass distribution for fission fragments from ^{252}Cf with high total kinetic energy.

69) S. Bjørnholm, Physics Scripta 10A, 110 (1974).

4. METEOROLOGY

The meteorology section is primarily engaged in studies of the planetary boundary layer. The efforts can be roughly classified as follows: micrometeorological research (4.1-4.6), climatological investigations (4.7-4.9), development of meteorological instruments (4.10-4.13), and applied meteorology (4.14-4.16).

The micrometeorological research aims at descriptions of the structure of atmospheric turbulence and its dependence on external parameters such as surface characteristics and the synoptic weather situation. An important goal is parameterization of the transport properties of atmospheric turbulence, so that the planetary boundary layer can be realistically incorporated in numerical weather prediction schemes.

At Risø a 120 m tower is available for experimental work. Meteorological variables such as wind speed and direction, temperature and humidity are measured routinely at a number of heights. As a result of the measurements, data records are available containing 17 years of hourly readings. The records are used extensively by the section and by others.

For field experiments the section has at its disposal a 50 m mobile tower and a data acquisition system installed in a van. The digital data system is capable of sampling 60 signals simultaneously at a rate of 200 times per second.

An experimental study is in progress of the influence of abrupt changes in surface roughness on the flow immediately above the surface (4.1). Three instrumented towers were put up along a line running inland at a right angle to the north shore of the Risø peninsula. They were in operation for about a year. In the fall of 1975 the experiment was moved to a similar but more ideal site on the other side of the Roskilde Fjord, where the terrain height difference between the beach and the land is less pronounced. Data were analyzed from an experiment in which detailed turbulence measurements were carried out in three heights along the Risø tower throughout 24 hours (4.2). Work was continued on a high-resolution model of the planetary boundary layer suitable for use with mesoscale dynamic models (4.3).

Air-sea interaction is a problem to which the section pays increasing attention (4.5-4.6). The interest is primarily concentrated on turbulence and fluxes in the lowest 20 m above the sea. The section participated in the Joint North Sea Wave Project (JONSWAP 1975) and in Project Kattegat-75.

The analysis of climatological data from Greenland, Risø and other locations in Denmark was continued (4.7-4.9). The meteorology section now operates 15 automatic meteorological observatories of which five in North Greenland are operated jointly with the Danish Meteorological Institute of special interest are in techniques of time-series modelling (4.7) and their applications to evaluation of climatic trends.

Work was continued on the development and testing of meteorological instruments and equipment (4.10-4.13) including the investigation of cup anemometer overspeeding, testing of a monostatic acoustic sounder, planning and design of automatic weather stations, and the development of methods for dynamic calibration of fine-wire resistance thermometers.

This year as earlier a number of tasks of an applied nature were undertaken (4.14-4.16). Experiments were carried out in order to obtain information on the dynamic response of bridges and other structures to fluctuating wind pressures. Other examples are: site evaluation for nuclear installations and assesment of wind power as an alternative energy source.

4.1 Flow over Non-Uniform Terrain

(N. E. Busch, K. Hedegaard, L. Kristensen, and E. W. Peterson (Oregon State University, U.S.A))

In the fall of 1974 a field experiment was started in order to study the effect on the wind-field of an abrupt change of the surface roughness. Three 13 m masts each carrying six cup anemometers, two thermometers, and one wind direction sensor were erected along a line perpendicular to the north shore of the Risø peninsula. The first mast was placed on the beach close to the shore line, the second 53 and the third 177 m inland. The two inland masts had similar base levels, 1.8 m higher than that of the mast on the beach. The terrain sloped somewhat unevenly from the first

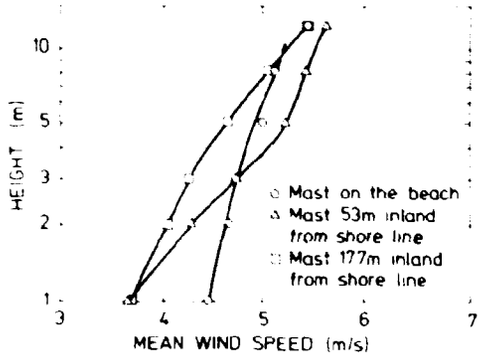

Fig. 24. Mean-wind profiles in the change-of-terrain-roughness experiment. Note that comparison between the profiles from the two masts closest to the coast show acceleration of the wind flow at the top and a corresponding slowing down at the lower levels.

mast to halfway between the first and the second mast thus producing a bluff with a height of 1.8 m. The measurements continued without interruption until August 1975. Twenty-eight periods of 100 minutes duration each satisfied the wind direction criterion that the wind should blow from the north, i.e., from a smooth to a rough surface. All cases show quite consistently a wind that accelerates from the first mast to the second mast at the top level (Fig.24). This acceleration, which overshadows the effect of the change in roughness, can only be attributed to the bluff mentioned above. An attempt to isolate the effect of the roughness change, by assuming that the static pressure field can be computed as if the flow were potential, shows profiles consistent with the Peterson model[70,71]. The experiment will be continued at a more ideal site on the Bognæs peninsula in Roskilde Fjord, where the difference in terrain height between the beach and the land is less pronounced.

4.2 Stress-Profile Experiment

(N. E. Busch, N. O. Jensen, and L. Kristensen)

In 1974 an experiment was performed in which detailed three-dimensional turbulence measurements were carried out at three heights (27, 60, and 94 m) along the Risø tower throughout 24 hours. The synoptic weather situation was very steady. A high pressure

---

70) E. W. Peterson, L. Kristensen, and Chang-Chung Su, Some Observations and Analysis of Wind over Non-Uniform Terrain. Submitted to Quart. J. Roy. Meteorol. Soc.

71) E. W. Peterson, Quart. J. Roy. Meteorol. Soc. 95, 561 (1969).

ridge over the North Sea moved very slowly towards the east. The data are therefore not masked by large-scale synoptic disturbances but show structural changes as a result of the diurnal cycle.

The data analysis, which has not yet been completed to the point that a final interpretation is possible, shows: a) that all variance spectra (based on half-hour time series) exhibit inertial subranges and indicate local isotropy for a high wave-number, b) that,at the lowest height, the peak scale for the logarithmic vertical velocity spectrum behaves as if the terrain were horizontally homogeneous and the flow-quasi-stationary[72]; so do σ_w/u_*, σ_v/u_*, and σ_u/u_* in spite of the fact that the Risø site is far from ideal; c) that the stress decreases unexpectedly rapidly with increasing height and generally disappears between 60 and 94 m, although the wind and temperature profiles are in accordance with generally accepted tower meteorology[73], and d) that the variances also decrease with increasing height but not as dramatically as the stress.

4.3 Simulation of Atmospheric Turbulence

(E. L. Petersen and J. A. Dutton (Pennsylvania State University, U.S.A.))

Work concerning an empirical turbulence model came to an end[74]. The objective was to derive a model possessing maximum simplicity and the minimum number of parameters consonant with representational adequacy. The model was created under the assumption that intermittency is a very important feature of turbulence, for which reason most effort was directed towards modelling this feature. This was accomplished by assuming that the intermittency of turbulence could be explained by considering turbulence to consist of intervals of passive turbulence and intervals of active turbulence. Measured turbulence data were then decomposed according to this assumption, and the proper orthogonal decomp-

---

72) N. E. Busch, Workshop on Micrometeorology., Amer. Meteorol. Soc., Boston (1973) 1.

73) H. A. Panofsky, ibid., 151.

74) E. L. Petersen, A Model for Simulation of Atmospheric Turbulence. Submitted to J. of Appl. Meteorol.

osition theorem was applied to the data thus giving statistical and sequential information about the passive and the active turbulence intervals. It was concluded that the model provides a practical, operational simulator of atmospheric turbulence.

4.4 Numerical Modelling of the Planetary Boundary Layer

(N. E. Busch, E. L. Petersen, R. A. Anthes*, and S. W. Chang*
(*Pennsylvania State University, U.S.A.))

The work with a simple planetary boundary layer (PBL) model[75,76] was continued and extended. The proposed prognostic equation for the mixing length λ (defined by $K_m = \lambda\sqrt{e}$)

$$\frac{\partial\lambda}{\partial t} = (\lambda_s - \lambda)/T,$$

where T is some characteristic time scale, may be written as

$$\frac{\partial\lambda}{\partial t} = \frac{\sqrt{e}}{a}\left(\frac{\sqrt{A}e}{u_*^2}(1-Rf)^{-\frac{1}{2}} - 1\right),$$

where A and a are assumed to be constants, $e = \frac{1}{2}\overline{u_i' u_i'}$ is the turbulent energy,

$$Rf = -(g/T_o)\,(\overline{\partial' w'}/P)$$

is the flux Richardson number, and $P = u_*^2\,|\partial \underline{V}/\partial z|$ is the mechanical production term. Furthermore, a simplified turbulent energy equation is used

$$\frac{\partial e}{\partial t} = P(1-Rf) - A\frac{e\sqrt{e}}{\lambda}.$$

The flux Richardson number Rf is related to the gradient Richardson number Ri through $Rf = (K_H/K_m)\,Ri$, and it is suggested that the ratio K_H/K_m of the vertical diffusivities for heat and momentum is related to the local flux Richardson number through

$$K_H/K_m = 1.35\,\frac{1-2Rf}{1-Rf}.$$

---

75) Risø Report No. 320, 80 (1974).

76) N. E. Busch, S. W. Chang, and R. A. Anthes, A High-Resolution Model of the Planetary Boundary Layer Suitable for Use with Mesoscale Dynamic Models. Submitted to J. Appl. Meteorol.

This suggestion is based on considerations of the simplified variance and heat-flux and variance budgets and on observations in the surface boundary layer.

It is interesting to note that the equations for λ and e when combined lead to a dissipation equation

$$\frac{\partial \varepsilon}{\partial t} = - \frac{\varepsilon}{2e} \left\{-3P(1-Rf) + \frac{2e\varepsilon}{\sqrt{A}au_*^2} \times (1-Rf)^{-\frac{1}{2}} - 2\varepsilon\left(\frac{1}{aA} - \frac{3}{2}\right)\right\}.$$

In quasi-stationary turbulence we are led to

$$\frac{e}{u_*^2} = A^{-\frac{1}{2}} \times \{1-Rf\}^{\frac{1}{2}},$$

since $\partial\lambda/\partial t = 0$. If we assume this to be approximately valid in general, the dissipation equation reduces to

$$\frac{\partial \varepsilon}{\partial t} = - \frac{\varepsilon}{2e} \{-3P(1-Rf) + 3\varepsilon\},$$

which may be compared to the suggestion by Wyngaard et al.[77],

$$\frac{\partial \varepsilon}{\partial t} = - \frac{\varepsilon}{2e} \{-3P(1-Rf) + 4\varepsilon\}.$$

The aim of work with these PBL models is not the development of high-order closure schemes but rather the development of the simplest possible PBL model that allows us to realistically model certain mesoscale phenomena - as, for instance, hurricanes.

4.5 Air-Sea Interaction (JONSWAP - 1975)

(N. E. Busch and S. E. Larsen)

The Joint North Sea Wave Project 1975 was carried out in the period June through September 1975 in continuation of the earlier JONSWAP experiments (JONSWAP 1968, 1970, and 1973). It took place west of the island of Sylt, and was coordinated by the Deutsches Hydrographisches Institut and Universität Hamburg, with financial support from the German Sonderforschungsbereich and NATO.

The experimental objectives of JONSWAP 1975 were essentially the same as for JONSWAP 1973: a) Investigation of the spatial and temporal structure of the surface wave field by means of instrumented aircraft and arrays of surface instruments, b) evaluation

77) J. C. Wyngaard, O. R. Coté, and K. S. Rao, Advances in Geo-Physics 18A, Academic Press, New York 747 (1974).

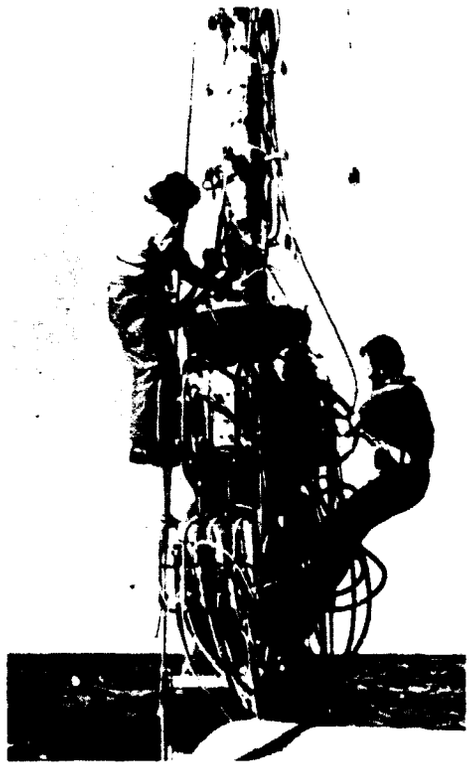

Fig. 25. Work on one of the instrumented masts during JONSWAP 1975. The picture shows the lower part of the mast, where the electronics containers were placed. The picture was taken during low tide, during high tide all containers were below the sea-surface.

of air-borne remote-sensing equipment versus ground-truth data, and c) investigation of air-sea interaction by means of detailed turbulence measurements in the lowest 15 m of the atmosphere above the sea. On the basis of experience and data from JONSWAP 1973, it was deemed unnecessarily complicated from a logistic point of view to aim at all three objectives simultaneously in JONSWAP 1975. Accordingly, the experiment was divided into two parts so that measurements concerning c) were carried out in June and July and measurements concerning a) and b) were carried out in August and September.

The Risø Meteorology Section participated in the parts of the experiment pertaining to c). With additional wave information coming from buoys within the experimental area, measurements were taken along two bottom-fast needles located 15 nautical miles off the coast of Sylt (Station 8-PISA), where the sea quantities measured were wave height and water temperature, while the atmospheric quantities measured were profiles of velocity, temperature and humidity, the three-dimensional turbulent velocity at three heights, and the turbulent temperature and humidity at one height.

The instrumentation employed was the same as during JONSWAP 1973 with a number of modifications which, based on experience from 1973, were made to facilitate the operation of the system under field conditions. The instrumentation consisted of: 1) a fast responding wind-vane equipped with a three-component hot-wire probe, a vertical hot-wire probe, and one cold-wire used as a resistance thermometer, 2) a Lyman-alpha humidiometer, 3) the necessary electronics encapsulated in two water-tight containers. The digital sampling system was operated with a scanning frequency corresponding to a sampling frequency of 200 Hz for all channels. Special care was taken to ensure good resolution of the signals over the whole frequency range. Measurements were made more or less continuously during three of the five weeks that the experiment lasted, with only short interruptions for repair and service of the equipment. This amounted to about 10^{10} data points sent by telemetry to the land-based receiver station on Sylt and recorded there.

The data are still in the process of being edited for analysis but from on-line surveillance and processing of the data-flow, the following tentative conclusions can be drawn: a) the data are generally of high quality, b) due to the land-sea-breeze circulation system that dominated the meteorological situation during a large part of the experiment, the data cover a very broad range of stability conditions. Apart from the usual problems with instrumentation and severe weather conditions, the worst problem encountered was huge flocks of seagulls that attacked and destroyed the sensors. The seagulls were eventually scared away by noisy men in rubber boats. In addition to the main experiment, a comparison was made between the instrumentation used by the Risø group and that used by the group from the University of Hamburg. Since the latter instrumentation was the key instrumentation in the flux-measurements during the 1974 GARP Tropical Experiment (GATE), this intercomparison is important for evaluation of the flux-data from GATE:

4.6 Air-Sea Interaction (Kattegat-1975)

(N. E. Busch, K. Hedegaard, and L. Kristensen)

As in 1973, the Section again cooperated with the Institute of Physical Oceanography, the University of Copenhagen, and the Institute of Geophysics, University of Bergen, on this project. A 40 m tower was erected in the Kattegat at the position $56^{o}38'N$, $12^{o}05'E$, and data including water currents and temperatures at several depths, were obtained through some two weeks. We were less involved in the experiment this year than in 1973. Measurements were made of wind speed, wind direction, and air temperature 15 m above the mean water level.

4.7 Climatology of Wind Direction Fluctuations

(L. Kristensen and H. A. Panofsky (Pennsylvania State University, U.S.A.))

The development of a high performance sine-cosine wind-direction sensor made it possible to apply an analogue variance-meter to the wind direction signals from Risø's 120 m tower. From late in 1974 routine measurements were made of the root mean square of the wind direction fluctuation, σ_D, at the 76 m level of this tower.

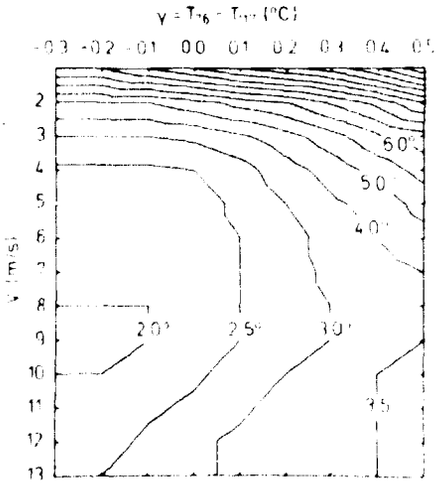

Fig. 26. Isopleth diagram $\sigma_D(\gamma,V)$. For increasing wind speed, σ_D approaches 3.5^{o} irrespective of the value of γ.

---

78) U. S. Safety Guide 23.

σ_D is closely related to the turbulent dispersion properties of the atmosphere, and it is particularly useful to compare σ_D statistically to the temperature lapse rate γ, which is often used as a turbulent dispersion index. The Risø tower data from the first half of 1975 were used in the comparison, in which also wind speed V and wind direction D were included[78]. Although westerly winds pass over the water and easterly winds do not, the σ_D showed no significant dependence on the mean wind direction. The analysis also showed that both γ and V influence σ_D (Fig.26). A two-dimensional average functional relationship $\sigma_D(\gamma,V)$ was established empirically. It was shown that about 37% of the total variance of σ_D could be accounted for by use of γ, based on temperature measurements at 76 and 117 m, and V, measured at 76 m as predictors. This corresponds to a multiple non-linear correlation coefficient of 0.61. It was not possible to develop a general theory based on the Risø tower data, and it must be stressed that the results cited apply to these only.

4.8 Climatology in Greenland

(N. E. Busch, G. Jensen, P. Dorph-Petersen*, and J. Taagholt*
(*Danish Meteorological Institute)).

Since 1972 five battery-powered dataloggers have been put into operation in North and Northeast Greenland in cooperation with the Danish Meteorological Institute and the Royal Danish Air Force. The reason for setting up these climatological stations or Unmanned Geophysical Observatories (UGOs) is the need for meteorological information from sites which may be chosen as locations for future manned stations. The locations and start-up times for the UGOs now in operation are given below:

NAME	GEOGRAPHICAL COORDINATES	START-UP
Nord	81°36'N, 16°40'W	June 1972
Kap Harald Moltke	82°09'N, 29°53'W	June 1973
Kap Morris Jesup	83°38'N, 33°22'W	July 1974
Polaris, Hall Land	81°43'N, 59°05'W	July 1975
Northwest Island, Carey Islands	76°38'N, 73°00'W	August 1975

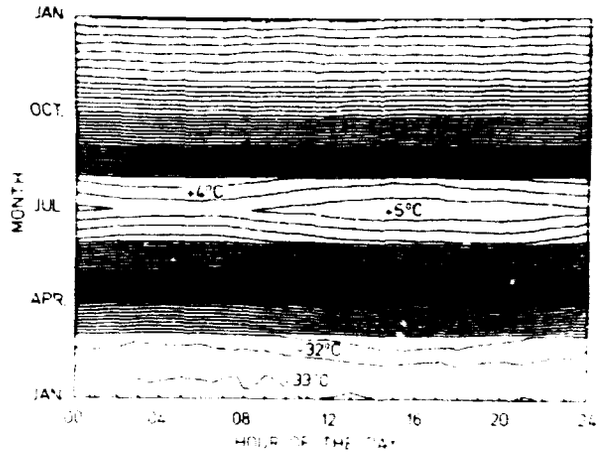

Fig. 27. Isopleth diagram from Kap Harald Moltke for the period 1973-1975. The average daily variation of the air temperature is shown as a function of the time of year.

Each UGO records pressure, air temperature, dew point, soil temperature, wind speed, and wind direction once every three hours. A detailed description of the UGOs and some of the recorded data have been published[79,80]. It may be of interest that the lowest air temperature measured by an UGO is -44.8°C (Nord) and the highest +13.9°C (Kap Harald Moltke). Figure 27 shows an example of an application of the recorded data.

4.9 Time Series Analysis

(S. E. Larsen and E. L. Petersen)

One of the most important techniques in time series analysis of geophysical data is spectral analysis with respect to frequency or wavenumber. For turbulence studies, the importance of spectral analysis is obvious since spectra reveal how the variance (or the co-variance) is distributed over wavenumbers and hence how the energy is distributed on scales. In recent years there has been increasing interest in improving methods for time series analysis and the research has largely been concerned with the identification problem of stochastic models for discrete time series.

We performed a study in order to judge the potential of the techniques of time series modelling with respect to the theoretical as well as the applied work undertaken by us. The first part of

the study dealt with the problems of fitting finite autoregressions to multivariable time series. The order of the autoregression was identified by means of Akaike's Information Criterion:[81]

$$AIC(m) = \log(\sigma_m^2) + 2m/T.$$

The value m minimizing the criterion is the selected order, σ_m^2 is the m-memory minimum mean square prediction error, and T the length of the time series. The second part of the study was devoted to the so-called Box-Jenkins Method[82]. The models which can be handled by this method are of the "Autoregressive-integrated-moving average" (ARIMA) form:

$$(1-\phi(1)B-\ldots-\phi(p)B^p)(1-B)^d z(t) =$$

$$(1-\theta(1)B-\ldots-\theta(q)B^q)a(t),$$

where z(t) is the time series, a(t) the white noise, B the back-shift-operator, $\phi(p)$ an autoregression of order p, and $\theta(q)$ is a moving average of order q. The models can further include seasonal and trend factors. Model building is a three-stage process: model identification, parameter estimation, and diagnostic checking.

The experience gained from analyses of several climatic time series (Fig. 28) indicates that the methods work well for model identification and prediction, although Akaike's criterion sometimes seems to be too conservative, i.e., choosing m too small. The fitted statistical models, if stationary, can be used directly to generate spectral estimates by simple calculations. However, when spectral estimation is the main objective, it is most efficiently achieved through calculating the periodiogram by means of fast Fourier transform procedures followed by an inspection of the periodiogram leading to a sensible smoothing.

---

79) L. Kristensen and J. Taagholt, Unmanned Geophysical Observatory at Nord in North Greenland, Danish Meteorological Institute, Copenhagen (1973).

80) G. Jensen, L. Kristensen, and J. Taagholt, Unmanned Geophysical Observatories in North Greenland 1973-1974, Danish Meteorological Institute, Copenhagen (1974).

81) H. Akaike, Ann. Inst. Statist. and Math. 23, 163 (1971).

82) G. E. P. Box and G. M. Jenkins, Time Series Analysis, Holden Day (1970).

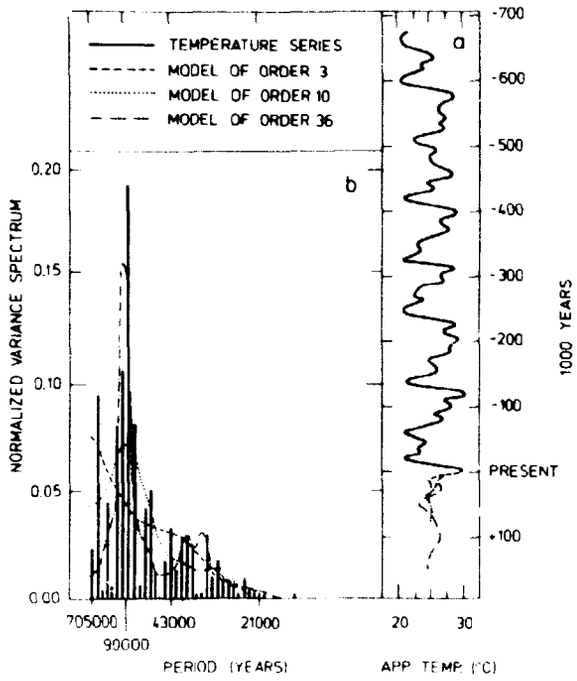

Fig. 28. a) Generalized temperature curve for the Entire Brunhe's epoch[83] with forecasts from three models. The solid line represents the temperature 700,000 years back based on air oxygen isotropic analysis of a long piston core from the western equatorial Pacific. The three broken curves show the development of the temperature in the future based on three autoregressive models of the order 3, 10, and 36 respectively. The calculations were performed on a discrete version of the temperature series with the time step equal to 5,000 years b) Periodogram of the temperature series and spectra of the three models. The excentricity of the Earth's orbit has a period of 90,000 years; also periods of 43,000 and 21,000 years can be argued from astronomical theories.

4.10 Development of an Automatic Weather Station (AWS)

(N. E. Busch, L. Kristensen, and P. Dorph-Petersen (Danish Meteorological Institute))

Development of an automatic weather station has been started by a group of Danish electronics firms. Financial support for building the prototype will be provided by the "Foundation for Support

---

83) C. Emiliani and N. J. Shackleton, Science 183, 511 (1974).

of Technological and Industrial Developments" under the Danish Ministry of Commerce. The meteorological design criteria were set up by a working group with members from Risø, the Danish Meteorological Institute and the military and civilian aviation meteorology services. The system consists of one or several low-powered sensor stations, which may be installed in hostile environments, one or several relatively high-powered local stations, each capable of collecting data from several sensor stations, and finally a central station to interrogate local stations where central supervision of a large area is essential. Communication will be established via telephone lines if possible or by means of broadband HF radio links if necessary. At the local station there will be options for recording of the data and also for preparation of the data in any special code (e.g. synop code). Prototypes of sensor stations and local stations will be available for testing in the spring of 1977.

4.11 Over-speeding in Cup Anemometers

(N. E. Busch, N. O. Jensen, and L. Kristensen)

The cup anemometer is the most commonly used instrument for horizontal wind speed measurements in connection with operational weather services of all kinds as well as in connection with climatological data collection. It is a simple and reliable instrument, whose alignment into the wind field is a matter of vertical positioning of the instrument axis once and for all. It was recognized very early that the operational principle behind the cup anemometer implies that it responds more quickly to an increase in wind speed than to a decrease of the same magnitude. This in turn means that a cup anemometer calibrated in a laminar wind flow will over-estimate the mean wind speed in a turbulent flow. An investigation of the problem was made by Schrenk[84], who developed a simple, non-linear model and made calculations for the case of sinusoidal fluctuations. Busch[85] found that the relative overspeeding must be proportional to the square of the turbulence intensity and determined the factor of proportion-

84) O. Schrenk, Z. Tech. Physik 10, 57 (1929).

85) N. E. Busch, Risø Report No. 99 (1965).

ality to be close to 0.4. An experimental determination of the over-speeding was carried out by Izumi and Barad[86]. They compared the signals from cup anemometers with those from an ultrasonic anemometer and concluded that a typical light-weight cup anemometer over-speeds by about 10% in the lowest 30 m of the atmosphere. A similar comparison made by us showed no detectable over-speeding. Thus, the situation appeared rather confusing, and a theoretical investigation was initiated. The preliminary result is that the relative over-speeding is equal to a sum of two terms of which one is proportional to the square of the vertical turbulence intensity. The other term is proportional to the square of the horizontal turbulence intensity and to the ratio between the instrument distance-constant and some length scale characteristic of the turbulence, to a power which probably lies between 2/3 and 1. Another and maybe more significant result of the investigation was that numerical calculations showed that over-speeding of a cup anemometer hardly ever exceeds a few per cent, except in cases with extreme turbulence intensities (>20%).

4.12 Acoustic Sounder

(N. O. Jensen and E. L. Petersen)

A monostatic acoustic sounder (acoustic radar) was installed at Risø near the 120 m meteorological tower in February 1975. The instrument continuously records information about stability, turbulence, and inversions in the lowest 500 m of the atmosphere. It transmits a brief pulse of sound upwards, listens to the echoes which return from temperature variations aloft, and displays the height of these echo regions on a chart. This instrument is the only one of its kind in Denmark although it is fairly cheap and has wide applications in environmental impact studies, real time emission control, diffusion research and synoptic and mesometeorological research.

In order to present the instrument and some of its potentials to technical circles in Denmark, we undertook a small air-pollution

---

86) Y. Izumi and M. L. Barad, J. Appl. Meteorol. 9, (1970).

case study[87]. The height of the mixed layer was estimated from the acoustic sounder record and used in a simple box model in order to predict the variation of the SO_2 concentration in Copenhagen throughout a particular day. The correspondence between the predicted and the measured SO_2 concentration was very good. One peculiar phenomenon observed on a record was analyzed[88] and interpreted as being associated with the passing of a land breeze front. A physical explanation of the frontal movements was suggested and the actual existence of the land breeze was demonstrated by examination of conventional meteorological observations.

4.13 Cold Wire Technique

(N. E. Busch, J. Højstrup, S. E. Larsen, and K. Rasmussen (The Technical University of Denmark))

The all dominating instrument in the measurement of small-scale turbulent temperature fluctuations is the cold-wire resistance thermometer. As the name indicates, this instrument measures temperature fluctuations by way of the associated resistance fluctuations in a small wire-probe. The limitations to the response characteristics of the instrument are solely due to the wire probe.

So far the standard technique for testing the response characteristics of the probe has been to study its response to temperature changes generated internally in the wire by modulation of the probe current. This type of test has confirmed the general belief that the probe essentially behaves as a low-pass filter with a flat transfer function up to a cut-off frequency mainly determined by the thermal inertia of the wire and the wind velocity. The drawback of this technique is that the probe responds to internally generated temperature variations, rather than to variations coming from the surrounding air. This means that various types of boundary layer around the wire prongs may affect the response characteristics differently in the measuring and the test situation. A calibration chamber was developed at the

---

87) E. L. Petersen and N. O. Jensen, Ingeniøren Nr. 9, 53 (1975).

88) E. L. Petersen and N. O. Jensen, A Mesoscale Phenomenon Revealed by an Acoustic Sounder. Submitted to J. Appl. Meteorol.

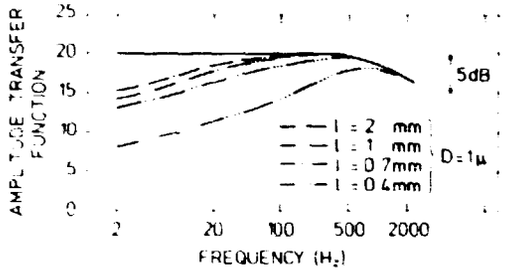

Fig. 29. Amplitude transfer functions versus frequency for four different cold-wires of diameter D and length ℓ. The solid line shows the expected behaviour of wires with D = 1 μm.

Acoustics Laboratory of the Technical University to rectify this drawback. In this chamber the air temperature is made to vary sinusoidally by means of a strong sound field. The amplitude of the temperature variation is typically about 0.1°C, and the frequency is variable between 2 Hz and 10 kHz. In this chamber transfer functions for cold-wire probes have been determined for probes with diameters ranging from 0.25 to 5 μm and lengths between 0.2 and 2 mm.

So far it has not been possible to develop a test chamber with a non-zero air velocity. With this limitation in mind, the following conclusions can be drawn: a) The upper cut-off frequency follows the expected dependence on wire diameter for diameters larger than about 1 μm. However, for diameter between 0.25 μm and 1 μm, the upper cut-off frequency seems to be independent of the diameter. b) The low-frequency part of the transfer functions deviates appreciably from the expected behaviour (Fig. 29). This deviation is believed to be caused by molecular heat conduction between an approaching temperature perturbation and the wire supports. The hypothesis is supported by the fact that the low-frequency parts of the transfer functions for all tested wires almost coincide when plotted versus frequency multiplied by the wire length squared, as should be expected if the phenomenon is governed by the Fourier heat-equation.

It seems impossible theoretically to generalize these results quantitatively to situations in which the flow-field has a non-zero mean-velocity. Therefore, it is planned to modify the calibration chamber to allow for such a flow within the chamber. However, the low-frequency deviations from the expected transfer

function lie precisely in the frequency interval where the current experimental evidence on the behaviour of turbulent fluctuations is somewhat confused. We therefore suggest that at least part of this confusion is caused by differences in sensor characteristics for the different types of cold-wire used to obtain the experimental results.

4.14 Dynamic Wind Loading

(N. E. Busch, O. Christensen, and N. O. Jensen)

In order to estimate the response of building structures to dynamic wind loading, it is of utmost importance to know the size and spatial distribution of the energy-containing eddies in the approaching turbulent wind field. One way of obtaining such information is by undertaking full-scale experiments involving simultaneous multiple-point wind vector measurements adjacent to an already existing structure. Statistical analysis of data from experiments of this kind should yield information concerning the coherence and phase between velocity components at different points, as functions of the separation between the points. The question of how a turbulent wind field excites structural response would be elucidated at the same time if this response was recorded together with the velocity recordings. Two experiments of this kind have been undertaken.

The Sotra Bridge Experiment [*)] took place during October and the first week of November as a joint experiment between SINTEF[+)], Trondheim, and Risø. The project focused on three-dimensional wind measurements at different points along the free span of a suspension bridge situated about 20 km from Bergen. In addition to the wind measurements, which were carried out by means of three ultrasonic anemometers, strain gauges and accelerometers were mounted to measure the response of the bridge to the wind. A total of 5 runs was made during the measuring period. The average wind speeds were between 10 and 15 m/s. Risø supplied the meteor-

---

[+)] Selskapet for Industriell og Teknisk Forskning, The Technical University of Norway.

[*)] Financed by the National Research Foundations of Norway and Denmark.

ological instruments and the data-logging equipment and was responsible for the recording of data and the preliminary analysis. SINTEF supplied the strain gauges and the accelerometers and will be responsible for the final analysis.

The Grosser Vogelsand Lighthouse Experiment**) was carried out in the last three weeks of November. Three-dimensional wind measurements were made adjacent to a lighthouse in the Bay of Helgoland (Fig. 30) in order to correlate the wind pressure on the structure to the turbulent wind. The measurements of wind pressure and structural response were carried out by a group from the Institut für Wasserbau III, Universität Karlsrhue. In connection with the experiment the structure of the internal boundary layer formed over a helicopter landing platform on top of the lighthouse was also investigated. A total of 9 runs was made under wind speeds ranging up to 25 m/s.

Fig. 30. Ultrasonic anemometer thermometer probe (Kaijo Denki, PAT 311) mounted on a horizontal boom reaching 7 m out from the center of the 4 m diameter shaft of the light house Grosser Vogelsand. The probe is placed 12 m above the sea. Another sonic probe was situated on a mast erected on the top of the light house, 55 m above the sea. Turbulence signals from these probes were recorded simultaneously with signals from accelerometers, showing the response of the tower structure to the wind gusts.

**) Supported by the Institut für Wasserbau III, Universität Karlsrhue, Germany.

The Meteorology Section participated in the work of the wind-load committee under the Dansk Ingeniørforning (Danish Society of Chemical, Civil, Electrical, and Mechanical Engineers). Work on the new Danish code for wind loading on structures is now complete and the code is expected to be made available for public criticism before the end of 1975. Compared to codes of other countries, the proposed Danish code is relatively advanced. Especially the chapter on design wind-profiles attracts attention, because it attempts to deal with the problems encountered over inhomogeneous terrain in a physically consistent way.

4.15 Applied Meteorology I: Site Evaluation

(N. E. Busch, K. Hedegaard, L. Kristensen, and S. E. Larsen)

The Section is engaged in the site evaluation and safety studies preceding the construction of the first nuclear power plants in Denmark. This year activities essentially concerned the following broad categories: a) General meteorological and climatological characteristics necessary for the evaluation of sites for various types and constructions of nuclear power plants. b) Statistical comparisons of dispersion characteristics from various sites with the primary aim of investigating to what extent the detailed climatological information available from measurements at Risø can form the basis for computing the consequences of radioactive releases at locations from which meteorological information is scarce or lacking. c) Models and computational procedures for estimating the consequences of radioactive releases originating from accidents as well as from routine operation. In this work the Section draws upon material made available by the Danish Meteorological Institute and on data collected from a number of automatically operated meteorological observatories established by the Section during the period 1973-1975. Site evaluation work is carried out in close cooperation with the Health Physics Department at Risø, which department, together with the Meteorology Section, hosted a joint Scandinavian Seminar on Nuclear Site Evaluation in April 1975.

4.16 Applied Meteorology II: Air Pollution Studies

(N. O. Jensen, S. E. Gryning *, and E. Lyck* (*Department of Health-Physics, Risø))

A substantial share of the air pollutants emitted in the urban environment originates from larger boiler plants. However, it is unlikely that a general abatement, say a decrease in the sulphur content of fuel oil, would be an optimal strategy in the economic sense, because the concentration contribution at a particular place, from a particular source, is not a function of the source strength alone. At present the concentration contribution cannot be assessed with sufficient accuracy by means of the calculation methods available for atmospheric dispersion. This is primarily because the crucial dispersion parameters are poorly known functions of topography and surface properties, in particular the aerodynamic surface roughness. Furthermore, their values are mainly based on observations made over rural terrain of diffusion from surface-based sources out to relatively short distances.

With this in mind, a feasibility study was undertaken[89,90] for the Danish Ministry of the Environment on "determination of atmospheric dispersion in the urban environment by means of tracers". The logistic requirements to the experimental set-up were established and plans for accomplishing such a study were outlined. Air samplers and meteorological instrumentation are currently under development. The first trial experiments are planned to take place in the spring of 1976.

---

89) N. O. Jensen, S. E. Gryning, and E. Lyck, Danish AEC (1975).

90) H. Flyger, N. O. Jensen, E. Lyck, S. E. Gryning, and J. Fenger Ingeniøren No. 12, 6 (1975).

5. LIQUID N_2 AND He PLANT

The production of liquid N_2 and He amounted to 200000 and 18500 litres respectively. Out of these amounts, 6000 litres of liquid He were delivered to laboratories in Copenhagen and Århus.

6. EDUCATIONAL ACTIVITIES AND PUBLICATIONS

Lectures

J. Als-Nielsen, Danmark's Energiforbrug og Atomkraft. "Energy Consumption and Atomic Power in Denmark"):
1) AOF/Risø, 3 meetings held in the Niels Bohr Auditorium at Risø.
2) Round Table, Sorø (October 1975).
3) Ingrid Jespersen's School, Copenhagen (November 1975).

J. Als-Nielsen, Dynamics of a Random Two-Dimensional Alloy. Brooknaven National Laboratory, New York (January 1975).

J. Als-Nielsen, Kernefysik (50 lectures on nuclear physics). Technical University of Denmark.

J. Als-Nielsen, Phase Transitions and Neutron Scattering. Technical University of Darmstadt, Germany (November 1975).

O. K. Andersen, (J. Madsen, U. K. Poulsen, and O. Jepsen), Volume and Structure Dependence of the Iron Magnetic Moment:
1) Kernforschungsanlage, Jülich, Germany (September 1975).
2) Chalmers Technical University, Göteborg, Sweden (October 1975).
3) University of Amsterdam, The Netherlands (December 1975).

B. Buras, Nuclear Methods in Solid State Physics (lecture series), University of Copenhagen.

N. E. Busch, A High-Resolution Model of the Planetary Boundary Layer Suitable for Use with Mesoscale Dynamic Models. National Center for Atmospheric Research, Colorado (April 1975).

N. E. Busch, Mesoscale Meteorology and Modelling. Atmospheric Sciences Laboratory, White Sands, New Mexico (April 1975).

N. E. Busch, A Simple, Time-Dependent Model of the Planetary Boundary Layer for Use in Hurricane Modelling. University of Washington, D. C. (April 1975).

N. E. Busch, Vejr, Klima og Luftforurening, ("Weather, Climate and Air Pollution"). University of Copenhagen (February 1975).

C. J. Christensen, Energi problemer. ("Problems in Energy Supply"). AOF/Risø meeting held in the Niels Bohr Auditorium at Risø, (September 1975).

C. J. Christensen, Ja eller nej til atomenergi? ("Yes or no to Atomic Power?"). Panel discussion on atomic power, Horsens Statsskole (March 1975).

N. O. Jensen (3 double lectures). Technical University of Denmark (October 1975):

1) Meteorologi og Aerodynamik i Relation til Luftforurening, ("Meteorology and Aerodynamics in Relation to Air Pollution").
2) Atmosfæriske Spredningsmekanismer og Modeller, ("Atmospheric Diffusion Mechanisms").
3) Røgfanemodeller, Anvendelser og Begrænsninger, ("Plume Dispersion Models, Applications and Limitations").

N. O. Jensen, Spredning i atmosfæren. ("Atmospheric Diffusion"). Course on environmental protection techniques held at the Technological Institute, Copenhagen (September 1975).

V. O. Jensen, Fusionsenergi (1). ("Fusion Energy (1)"). Lecture broadcast by Radio Denmark, January 22, 1975.

V. O. Jensen, Fusionsenergi (2). ("Fusion Energy (2)"). Lecture broadcast by Radio Denmark, November 1, 1975.

V. O. Jensen, Plasmafysik og Fusionsforskining (40 double lectures on plasma physics and fusion research). Technical University of Denmark.

J. K. Kjems, Physics of Adsorbed Atoms and Molecules. University of Aarhus (January 1975).

L. Kristensen, Automatic Climatological Measurements in North Greenland:
1) Pennsylvania State University, Pennsylvania (February 1975).
2) Oregon State University, Oregon (February 1975).
3) AIDJEX Office, Seattle, Washington (March 1975).

L. Kristensen, Some Aspects of the Application of Digital Techniques to Stochastic Time Series. Pennsylvania State University, Pennsylvania (February 1975).

B. Lebech, (K. A. McEwen, and P.-A. Lindgård), Magnetism in Prasedodymium-Neodymium Single Crystal Alloys.
1) Adam Mickiewics University, Poznan, Poland (November 1975).
2) Jagiellonian University, Cracow, Poland (November 1975).

B. Lebech (and P.Å. Hansen), Magnetic Structures of Tb-Tm Single Crystal Alloys. Adam Mickiewics University, Poznan, Poland (November 1975).

B. Lebech, (B. D. Rainford, and B. Buras), Inelastic Neutron Scattering from Cerium Under Pressure. Adam Mickiewics University, Poznan, Poland (November 1975).

P.-A. Lindgård, The Magnetic Properties of the Rare Earth Metals. (4 lectures), Iowa State University, Ames Iowa (October 1975).

P.-A. Lindgård, Theory of Anisotropic Magnetic Alloys:
1) Chalk River, Canada (October 1975).
2) Northwestern University, Evanston, Illinois (October 1975).
3) Iowa State University, Ames, Iowa (October 1975).

P.-A. Lindgård, Phase Diagrams and Magnetic Excitations in Rare Earth Metals and Alloys:
1) Oak Ridge National Laboratory, Tennessee (December 1975).
2) Rutgers University, New Jersey (December 1975).
3) Brookhaven National Laboratory, New York (December 1975).

H. Bjerrum Møller, Magnetiske Excitationer. ("Magnetic Excitations"). Solid State Physics Course arranged by the Danish Society for the Physics and Chemistry of Condensed Matter, 3 lectures given at the H. C. Ørsted Institute, Copenhagen (January 1975).

M. Nielsen, Fononer ("Phonons"). 2 lectures given at the Solid State Physics course arranged by the Danish Society for the Physics and Chemistry of Condensed Matter at the H. C. Ørsted Institute, Copenhagen (January 1975).

H. L. Pécseli, Landau-Damping and Instabilities in a Collisionless Plasma. The Danish Space Research Institute, Lyngby (November 1975).

E. L. Petersen, Spredning i atmosfæren. ("Atmospheric Diffusion"). Course in environmental protection techniques at the Technological Institute, Copenhagen (October 1975).

H. Sørensen, The Deuterium Film Experiment. The Max-Planck-Institute, Garching, Germany (February 1975).

Publications

J. Als-Nielsen, R. J. Birgeneau, H. J. Guggenheim, and G. Shirane, Spin Dynamics and Critical Fluctuations in a Two-Dimensional Random Antiferromagnet. Phys. Rev. B12, (1975) 4963-4979.

J. Als-Nielsen, L. M. Holmes, F. Krebs-Larsen, and H. J. Guggenheim, Spontaneous Magnetization in the Dipolar Ising Ferromagnet $LiTbF_4$. Phys. Rev. B12, (1975) 191-197.

J. Als-Nielsen and J. K. Kjems, Measurements of the Flux from the Cold Source at DR3. Risø-M-1802 (1975) 7 pp.

O. K. Andersen, Linear Methods in Band Theory. Phys. Rev. B12, (1975) 3060-3083.

M. M. Beg, Growing of Single Crystals of Lithium. Risø-M-1791 (1975) 11 pp.

R. J. Birgeneau, L. R. Walker, H. J. Guggenheim, J. Als-Nielsen and G. Shirane, Excitations in a Two-Dimensional Random Antiferromagnet. J. Phys. C: Solid State Physics 8, (1975) L328-L333.

S. Boisen Fritz-Rasmussen, C. J. Christensen, C. U. Linderstrøm-Lang, H. Neltrup, I. Rasmussen, and B. Vigeholm, Alternativ energiforskning. ("Alternative Energy Research"). Risø-M-1834 (1975) 34 pp.

B. Buras, Time-of-Flight Diffractometry. Physical Laboratory II, University of Copenhagen Monograph No. 75-13, (1975), 43 pp. and proceedings of the Neutron Diffraction Conference, Petten, The Netherlands, 5-6 August 1975, RCN-234 (1975) 307-346.

B. Buras and L. Gerward, Relations between Integrated Intensities in Crystal Diffraction Methods for X-rays and Neutrons, Acta Cryst. A31, (1975) 372-374.

B. Buras, J. Staun Olsen, L. Gerward, B. Selsmark, and A. Linde:aard Andersen, Energy-Dispersive Spectroscopic Methods Applied to X-ray Diffraction in Single Crystals. Acta Cryst. A31, (1975) 327-333.

C. T. Chang, The Magnetic Shielding Effect of a Refuelling Pellet. Nuclear Fusion 15, (1975) 595-604.

C. J. Christensen, Om Risikoen ved at undvære Atomenergi. Weekend avisens kronik ("The Dangers of not Utilizing Atomic Power"), newspaper article, 7 February 1975.

R. A. Cowley, O. W. Dietrich, and D. A. Jones, Magnetic Excitations of Mixed CoF_2/ZnF_2 Crystals. J. Phys. C: Solid State Phys. 8, (1975) 3023-3035.

N. D'Angelo, P. Michelsen, H. L. Pécseli, and P. I. Petersen, The K-Spectrum of Ionospheric Irregularities, J. Geophys. Res. 80, (1975) 1854-1855.

N. D'Angelo, P. Michelsen, and H. L. Pécseli, Damping-Growth Transition for Ion-Acoustic Waves in a Density Gradient. Phys. Rev. Lett. 34 (1975) 1214-1216.

O. W. Dietrich, A. J. Henderson, and H. Meyer, Spin-Wave Analysis of Specific Heat and Magnetization in EuO and EuS. Phys. Rev. B12, (1975) 2844-2855.

O. W. Dietrich, G. A. Mackenzie, and G. S. Pawley, The Structural Phase Transition in Solid DCN. J. Phys. C: Solid State Phys. 8, (1975) L98-L102.

O. W. Dietrich, G. Meyer, R. A. Cowley, and G. Shirane, Line Shape of the Magnetic Excitations in Substitutionally Disordered Antiferromagnets. Phys. Rev. Lett. 35, (1975) 1735-1738.

D. Dimock, K. Jensen, V. O. Jensen, L. W. Jørgensen, H. L. Pécseli, H. Sørensen, and F. Øster, Pellet Acceleration. Studies Relating to the Refuelling of a Steady-State Fusion Reactor. Risø Report No. 332 (1975) 20 pp.

H. Flyger, N. O. Jensen, E. Lyck, S. E. Gryning, and J. Fenger, Forurening fra Høje skorstene skal nu undersøges af Risø ("The Pollution from Tall Stacks will now be Investigated by Risø") , Ingeniøren No. 12 (1975) 6-7.

F. Yssing Hansen, T. Steen Knudsen, and K. Carneiro, Structure of Amorphous Selenium studied by Neutron Diffraction. J. Chem. Phys. 62, (1975) 1556-1565.

L. M. Holmes, H. J. Guggenheim, and J. Als-Nielsen, Neutron Study of Crystal-Field Excitations in $LiTbF_4$. Proceedings of the International Conference on Magnetism, Moscow, 1973, 6, (1974) 256-261.

L. M. Holmes, J. Als-Nielsen, and H. J. Guggenheim, Dipolar and non-Dipolar Interactions in $LiTbF_4$. Phys. Rev. B12, (1975) 180-190.

J. G. Houmann, M. Chapellier, A. R. Mackintosh, P. Bak, O. D. McMasters, and K. A. Gschneidner, Jr., Magnetic Excitations and Magnetic Ordering in Praseodymium. Phys. Rev. Lett. 34, (1975), 587-590.

J. G. Houmann, J. Jensen, and P. Touborg, Spin Waves in Terbium. III, Magnetic Anisotropy at Zero Wave Vector, Phys. Rev. B12, (1975) 332-344.

J. Jensen and J. C. Gylden Houmann: Anisotropic Exchange Interaction Between the Magnetic Ions in Terbium. Proceedings of the International Conference on Magnetism, Moscow, 1973, 6, (1974), 242-246.

J. Jensen, J. C. G. Houmann, and H. Bjerrum Møller, Spin Waves in Terbium. I. Two-Ion Magnetic Anisotropy. Phys. Rev. B12, (1975) 303-319.

J. Jensen and J. C. G. Houmann, Spin Waves in Terbium. II, Magnon-Phonon Interaction. Phys. Rev. B12, (1975) 320-331.

N. O. Jensen, Beregning af spredning i atmosfæren. ("Atmospheric Diffusion" In: Lecture notes for course in environmental protection techniques). Kompendium for Miljøværnskursus, Technological Institute, Copenhagen (1975).

N. O. Jensen, S. E. Dryning, and E. Lyck, Projektforslag: Undersøgelse af et sporstofs udbredelse fra en høj skorsten i et byområde ("A Feasibility Study for the Danish Ministry of the Environment on the Determination of Atmospheric Dispersion in the Urban Environment by Means of Tracers"). Danish Atomic Energy Commission Research Establishment, Risø, (1975) 40 pp.

V. O. Jensen, Laserfusion ("Laser Fusion"). Fysisk Tidsskrift 73, (1975) 45-47.

L. W. Jørgensen, Fast brint - plasma vekselvirkning. En undersøgelse i relation til brændstoffødning af fusionsreaktorer. ("Solid Hydrogen-Plasma Interaction. A Study in Relation to Refuelling of Fusion Reactors"), Risø-M-1823 (1975) 75 pp.

J. Jepsen, Electronic Structure and Magnetic Breakdown in Titanium. Phys. Rev. B12, (1975) 2988-2997.

J. Jepsen, O. K. Andersen, and A. R. Mackintosh, The Electronic Structure of hcp Transition Metals, Phys. Rev. B12, (1975) 3084-3103.

L. W. Jørgensen, A. H. Sillesen, and F. Øster, Ablation of Hydrogen Pellets in Hydrogen and Helium Plasmas. Plasma Phys. 17, (1975) 453-461.

J. K. Kjems, J. Als-Nielsen, and H. Fogedby. Spin Wave Dispersion in $CoCl_2$-$2D_2O$: A System of Weakly Coupled Ising Chains. Phys. Rev. B12, (1975) 5190-5197.

J. K. Kjems and G. Dolling: Crystal Dynamic of Nitrogen: The Cubic-Phase. Phys. Rev. B11, (1975) 1639-1697 (Work performed at Brookhaven National Laboratory under the auspices of the USAEC).

J. K. Kjems, W. Hayes, and S. H. Smith, Wavevector Dependence of the Jahn-Teller Interactions in $TmVO_4$. Phys. Rev. Lett. 35, (1975) 246-253.

L. Kristensen, Automatic Climatological Measurements in North Greenland. Proceedings of a WMO Technical Conference on Automated Meteorological Systems (TECAMS), WMO-No. 420, Washington, D.C. (1975) 246-253.

B. Lebech, K. A. McEwen, and P.-A. Lindgård, Magnetism in Praseodymium-Neodymium Single-Crystal Alloys. J. Phys. C: Solid State Phys. 8, (1975) 1684-1696.

B. Lebech and M. Nielsen, Intensity and Resolution of a General Scan in Reciprocal Space. Proceedings of the Neutron Diffraction Conference, Petten, The Netherlands, 5-6 August 1975, RCN-234 (1975) 466-486.

J. Leth and J. Als-Nielsen, Kolde neutroner - et vigtigt værktøj i den faststoffysiske forskning, I og II ("Cold Neutrons - An Important Tool in Solid State Physics, I and II"). Ingeniøren No. 5, 24-25 (1975) and Ingeniøren No. 6, 33-35 (1975).

P.-A. Lindgård, Calculation of Spectra Solids, Solid State Commun. 16, (1975) 481-484.

P.-A. Lindgård, Renormalization of Magnetic Excitations in Praseodymium. J. Phys. C: Solid State Phys. 8, (1975) L178-L181.

P.-A. Lindgård, Tables of Products of Tensor Operators and Stevens Operators. J. Phys. C: Solid State Phys. 8, (1975) 3401-3407.

P.-A. Lindgård, J. Als-Nielsen, R. J. Birgeneau, and H. J. Guggenheim, Spin Wave Dispersion and Magnetization in $NiCl_2$. Proceedings of the International Conference on Magnetism, Moscow 1973, 5, (1974) 575-580.

P.-A. Lindgård and P. Bak, Magnetic Properties of Nd-Pnictides. Proceedings of the International Conference on Magnetism, Moscow 1973, 1(2), (1974) 99-103.

P.-A. Lindgård, R. J. Birgeneau, J. Als-Nielsen, and H. J. Guggenheim, Spin Wave Dispersion and Sublattice Magnetization in $NiCl_2$. J. Phys. C: Solid State Phys. 8, (1975) 1059-1069.

P.-A. Lindgård, B. N. Harmon, and A. J. Freeman, Theoretical Magnon Dispersion Curves for Gd. Phys. Rev. Lett. 35, (1975) 383-386.

G. A. Mackenzie, G. S. Pawley, and O. W. Dietrich, Neutron Powder Diffraction Analysis and Constrained Refinement of Per-Fluorodiphenyl. Acta. Cryst. A31, (1975) 851-852.

H. B. Møller and T. Riste, Neutron Scattering Study of Transitions to Convection and Turbulence in Nematic Para-azoxyanisole. Phys. Rev. Lett. 34, (1975) 996-999.

H. B. Møller, T. Riste, and K. Otnes, Neutron Scattering Study of Transitions to Convection and Turbulence in Nematic Para-Azoxyanisole (PAA). In: Fluctuations, Instabilities, and Phase Transitions. ed. by T. Riste (Plenum Press, New York (1975)) 313-322.

M. Nielsen and W. D. Ellenson, H_2 and D_2 Adsorbed on Graphite Studied by Neutron Scattering. Proceedings of the 14th International Conference on Ion Temperature Physics, Otaniemi, Finland 4, (1975) 437-440.

M. Nielsen, W. Ellenson, S. Shapiro, and K. Carneiro, Inelastic Neutron Scattering from Molecular Hydrogen. Fizika Nizkich Temperatur 1, (1975) 770-777.

G. S. Pawley and O. W. Dietrich: A Phase Transformation with No Change in Space Group Symmetry: Octafluoronaphtalene, J. Phys. C: Solid State Phys. 8, (1975) 2549-2558.

H. L. Pécseli, Instability Caused by Dissipation in Plasmas carrying Negative Energy Waves, Plasma Phys. 17, (1975) 493-497.

H. L. Pécseli, Ion Acoustic Waves in the Presence of High Frequency Oscillations. Risø-M-1790, (1975) 19 pp.

H. L. Pécseli, Propagation of Ion Acoustic Perturbations. Physica Scripta 11, (1975) 311-315.

H. L. Pécseli, Stabilization of the Ion Acoustic Instability by High Frequency Oscillations. Phys. Lett. A53, (1975) 491-492.

E. L. Petersen, On the Kinetic Energy Spectrum of Atmospheric Motions in the Planetary Boundary Layer. Risø Report No. 285 (1975) 103 pp.

E. L. Petersen and N. O. Jensen, Atmosfærisk ekkolod på Risø kan varsle farlige luftforurenings situationer ("Acoustic Sounder. New Meteorological Instrument at Risø with Special Application to Air Pollution Monitoring"). Ingeniøren No. 9 (1975) 53-54.

J. Juul Rasmussen and H. L. Pécseli, Electromagnetic Radiation Originating from Unstable Electron Oscillation. Phys. Lett. 55A (1975) 85-86.

I. K. Robinson, A Study of a Position Sensitive Neutron Detector, Risø-M-1824 (1975) 38 pp.

L. W. Roeland, G. J. Cock, and P.-A. Lindgård, High Field Magnetization of Tb Single Crystal, J. of Phys. C: Solid State Phys. 8, (1975) 3427-3438.

S. M. Shapiro and P. Bak, Crystal Field Parameter and Phase Transitions in ErSb. J. Phys. Chem. Solids 36. (1975) 579-581.

H. G. Smith, M. Nielsen, and C. B. Clark, Lattice and Molecular Vibrations in Single Crystal I_2 at 77 K by Inelastic Neutron Scattering. Chem. Phys. Lett. 33, (1975) 75-78.

J. Taagholt, L. Kristensen, and G. Jensen, Danske automatiske meteorolgiske stationer i Nord-og Nordøstgrønland ("Automated Danish Meteorological Observatories in North and Northeast Greenland"), Grønland, No. 5, (1975) 129-133.

H. Taub, L. Passell, J. K. Kjems, K. Carneiro, J. P. McTague, and J. G. Dash, Neutron Scattering Studies of the Structure and Dynamics of ^{36}Ar Monolayer Films Adsorbed on Basal Plane Oriented Graphite. Phys. Rev. Lett. 34, (1975) 654-657 (Work performed at Brookhaven National Laboratory under the auspices of the USAEC).

E. Warming, L. P. Kayn, B. Lippold, M. M. Lukina, E. Mattiss, B. Matz, K. Feldmann, and K. Henning. Crystal Field Levels in $PrFeO_3$ and $PrGaO_3$. JINR P14-8728 (1975) 13 pp.

E. Warming and P. Bak. Crystal Field Splittings of NdN. J. Phys. C: Solid State Phys. 8, (1975) 1054-1058.

J. Wenzel, C. U. Linderstrøm-Lang, and S. A. Rice., Amorphous Solid Water: A Neutron Diffraction Study. Science 187, (1975) 428-430.

Conference Contributions

J. Als-Nielsen, Critical Fluctuations in the Dipolar Coupled Ising Ferromagnet. Gordon Conference on Critical Phenomena, New Hampshire, August 1975.

J. Als-Nielsen, Dynamics and Critical Fluctuations of a Random Two-Dimensional System. 3rd Annual Meeting of the Danish Physical Society, Lyngby 28-29 November 1975.

J. Als-Nielsen, R. J. Birgeneau, H. J. Guggenheim, and G. Shirane, Dynamics of a Random Two-Dimensional Alloy. Danish Society for the Physics and Chemistry of Condensed Matter. General Meeting, Rungsted, 20-22 May 1975.

J. Als-Nielsen, R. J. Birgeneau, and G. Shirane, Spin Dynamics and Critical Fluctuations of a Site-Random, Two-Dimensional Antiferromagnet $Rb_2Mn_{0.5}Ni_{0.5}F_4$. 21st Annual Conference on Magnetism and Magnetic Materials, Philadelphia, Pennsylvania, 9-12 December 1975.

O. Alstrup, L. Gerward, B. Selsmark, B. Buras, and J. Staun Olsen, Polarization of X-rays from a Thick Target and its Influence on Integrated Intensities of Bragg Reflections. Danish Society for the Physics and Chemistry of Condensed Matter. General Meeting, Rungsted 20-22 May 1975.

O. Alstrup, L. Gerward, B. Selsmark, B. Buras, and J. Staun Olsen, Polarization of X-rays from a Thick Target and its Influence on Integrated Intensities of Bragg Reflections. 10th International Congress of Crystallography, Amsterdam, The Netherlands, 7-15 August 1975.

A. A. Ballman, L. M. Holmes, F. Krebs-Larsen, B. Lebech, and O. V. Nielsen, Nuclear Structure and Magnetic Properties of $MnNb_2O_6$. 10th International Congress of Crystallography, Amsterdam, The Netherlands, 7-15 August 1975.

B. Buras, Time-of-Flight Diffractometry. Neutron Diffraction Conference, Petten, The Netherlands, 5-6 August 1975.

B. Buras, W. D. Ellenson, B. Lebech, and S. M. Shapiro, High Pressure Neutron Diffraction Studies of Paratellurite and Chromium. Danish Society for the Physics and Chemistry of Condensed Matter. General meeting, Rungsted, 20-22 May 1975.

B. Buras, W. D. Ellenson, B. Lebech, and S. M. Shapiro, High Pressure Neutron Diffraction Studies of Structural and Magnetic Phase Transitions. Electronic Properties of Solids under High Pressure, Leuven, Belgium, 1-5 September 1975. In: Euro-Physics Conference Abstracts 1A, (1975) 81-82.

B. Buras, J. Staun Olsen, L. Gerward, B. Selsmark, and A. Lindegaard Andersen, Energy-Dispersive Spectroscopic Methods Applied to X-ray Diffraction in Single Crystals. Danish Society for the Physics and Chemistry of Condensed Matter. General meeting, Rungsted, 20-22 May 1975.

N. E. Busch, Design, Response Characteristics, Calibration and Performance of a Three-Dimensional Hot-Wire System for Use in the Atmosphere. European Mechanics Colloquium 63, The Technical University of Denmark, 20-22 August 1975.

N. E. Busch, Fluxes in the Surface Boundary Layer over the Sea. Advanced Study Institute on Modelling and Prediction of the Upper Layers of the Ocean, Sogesta, Italy, 8-19 September 1975.

C. T. Chang, The Effect of Turbulent Transport on the Solution Rate of a Refuelling Pellet. 5th European Conference on Controlled Fusion and Plasma Physics, Lausanne, Switzerland, 1-5 September 1975.

O. W. Dietrich, R. A. Cowley, and G. Meyer, Magnetic Excitations in Random Magnets: CoF_2/ZnF_2 and MnF_2/ZnF_2. Danish Society for the Physics and Chemistry of Condensed Matter. General meeting, Rungsted, 20-22 May 1975.

P. Å. Hansen and B. Lebech, Magnetic Properties and Structures of Tb-Tm Alloys Determined by Neutron Diffraction. 10th International Congress of Crystallography, Amsterdam, The Netherlands, 7-15 August 1975.

F. Højstrup, K. Rasmussen, and S. E. Larsen, Determination of Response Characteristics of Wire-Probes, Used in Resistance Thermometry, by Means of Sound Generated Temperature Fluctuations. European Mechanics Colloquium, The Technical University of Denmark, 20-22 August 1975.

J. C. G. Houmann, M. Chapellier, A. R. Mackintosh, B. D. Rainford, P. Bak, O. D. McMasters, and K. A. Gschneidner, Jr., Magnetic Excitations and Magnetic Ordering in Praseodymium. Danish Society for the Physics and Chemistry of Condensed Matter. General meeting, Rungsted, 20-22 May 1975.

N. O. Jensen, On the Lay-out for a Single Source Atmospheric Dispersion Experiment in an Urban Area. Meeting on the COST 61a Project at the KEMA Institute, Arnhem, The Netherlands, 14-17 May 1975.

V. O. Jensen and P. Michelsen, A Green's Function Study of Absolute and Convective Ion Beam Instabilities. 2nd International Congress on Waves and Instabilities in Plasmas, Innsbruck, Austria, 17-21 April 1975.

O. Jepsen, Calculations on the Electronic Spectrum. 5th Annual Symposium on Electronic Structure of Metals and Alloys. Dresden, D. D. R., 20-26 April 1975.

O. Jepsen and O. K. Andersen, Crystal Structures of Non-Magnetic Transition Metals. Danish Society for the Physics and Chemistry of Condensed Matter. General meeting, Rungsted, 20-22 May 1975.

O. Jepsen, A. R. Mackintosh and O. K. Andersen, The Electronic Structure of hcp Transition Metals. Danish Society for the Physics and Chemistry of Condensed Matter. General meeting Rungsted, 20-22 May 1975.

L. W. Jørgensen, Determination of the Ion Velocity for a Rotating Plasma by Measuring of the Doppler Broadening. Plasma og Gasutladningsymposiet, Geilo, Norway, 5-8 February 1975.

J. K. Kjems, J. Als-Nielsen, and H. Fogedby, Spin Wave Dispersion in $CoCl_2$-$2D_2O$: A System of Weakly Coupled Ising Chains. Danish Society for the Physics and Chemistry of Condensed Matter. General meeting, Rungsted, 20-22 May 1975.

J. K. Kjems and G. Dolling, Correlation Effects Above the $\alpha - \beta$ Transition in Solid Nitrogen. NATO Advanced Study Institute, Geilo, Norway, 11-20 April 1975.

J. K. Kjems, K. Carneiro, L. Passell, H. Taub, G. Dash, and J. P. McTague, Structure and Dynamics of ^{36}Ar Monolayer Films Adsorbed on Grafoil. Meeting of the Faraday Society Oxford, U. K., 7-8 July 1975.

J. K. Kjems, L. Passell, H. Taub, and G. Dash, Neutron Diffraction from N_2 Adsorbed on Grafoil. Meeting of the Faraday Society, Oxford, U.K., 7-8 July 1975.

L. Kristensen, Automatic Climatological Measurements in North Greenland. Technical Conference on Automated Meteorological Systems (TECAMS), Washington, D.C., 14-19 February 1975.

B. Lebech, K. A. McEwen, and P.-A. Lindgård, Magnetism in Praseodymium-Neodymium Single Crystal Alloys. Danish Society for the Physics and Chemistry of Condensed Matter. General meeting, Rungsted, 20-22 May 1975.

B. Lebech and M. Nielsen, Intensity and Resolution of a General Scan in Reciprocal Space. Neutron Diffraction Conference, Petten, The Netherlands, 5-6 August 1975.

P.-A. Lindgård, Multicritical Points in Anisotropic Mixtures. NATO Advanced Study Institute, Geilo, Norway, 11-20 April 1975.

P.-A. Lindgård, Multicritical Points in Anisotropic Mixtures. Danish Society for the Physics and Chemistry of Condensed Matter. General meeting, Rungsted, 20-22 May 1975.

P.-A. Lindgård, Theory of Anisotropic Magnetic Alloys. 21st Annual Conference on Magnetism and Magnetic Materials, Philadelphia, Pennsylvania, 9-12 December 1975.

G. A. Mackenzie, G. S. Pawley, and O. W. Dietrich, Neutron Powder Diffraction Analysis and Constrained Refinement of Molecular Crystals. Danish Society for the Physics and Chemistry of Condensed Matter. General meeting, Rungsted, 20-22 May 1975.

G. A. Mackenzie, G. S. Pawley, and O. W. Dietrich, The Structural Phase Transition in Solid DCN, 12th European Conference of Molecular Spectroscopy, Strasbourg, France, 1-4 July 1975.

G. A. Mackenzie, G. S. Pawley, and O. W. Dietrich, Neutron Powder Diffraction Analysis and Constrained Refinement of Molecular Crystals. 10th Annual Conference of Crystallography. Amsterdam, The Netherlands, 7-15 August 1975.

J. Madsen and O. K. Andersen, Volume and Structure Dependence of the Iron Magnetic Movement. Danish Society of the Physics and Chemistry of Condensed Matter. General meeting, Rungsted, 20-22 May 1975.

J. Madsen, O. K. Andersen, U. K. Poulsen, and O. Jepsen, Canonical Band Theory of the Volume and Structure Dependence of the Iron Magnetic Movement. 21st Annual Conference on Magnetic Materials, Philadelphia, Pennsylvania, 9-12 December 1975.

G. M. Meyer and O. W. Dietrich, Neutron Scattering Studies on CsDA, Third European Meeting on Ferroelectricity, Zurich, Switzerland, September 1975.

P. Michelsen, Pulse Propagation in an Unstable Q-Machine Plasma. 2nd International Congress on Waves and Instabilities in Plasmas, Innsbruck, Austria, 17-21 March 1975.

P. Michelsen, Ion Acoustic Waves in a Density Gradient. 7th European Conference on Controlled Fusion and Plasma Physics, Lausanne, Switzerland, 1-5 September 1975.

H. Bjerrum Møller, Crystal Field Exchange Anisotropy in Rare Earth Metals, 12th Annual Solid State Physics Conference, Manchester, U. K., 6-8 January 1975.

H. Bjerrum Møller and T. Riste, Neutron Scattering Study of Transitions to Convection and Turbulence in Nematic Para-azoxyanisole. NATO Advanced Study Institute on Physics of Non-equilibrium Systems, Geilo, Norway. 11-20 April 1975.

H. Bjerrum Møller and T. Riste, Neutron Diffraction Study of the Onset of Turbulence in Nematic Para-azoxyanisole. Danish Society for the Physics and Chemistry of Condensed Matter. General meeting, Rungsted, 20-22 May 1975.

M. Nielsen and W. Ellenson, The Structure of and the Dynamics of H_2 and D_2 Adsorbed on Graphite Studied by Neutron Scattering. Danish Society for the Physics and Chemistry of Condensed Matter. General meeting, Rungsted, 20-22 May 1975.

M. Nielsen and W. D. Ellenson, H_2 and D_2 Adsorbed on Graphite Studied by Neutron Scattering. 14th International Conference on Low Temperature Physics, Otaniemi, Finland, 14-20 August 1975.

H. L. Pécseli, Ion Acoustic Waves in a Density Gradient. Plasma og Gasuldladningsymposiet, Geilo, Norway, 5-8 February 1975.

H. L. Pécseli, Experimental Investigations of the Farley Instability. 2nd International Congress on Waves and Instabilities in Plasmas, Innsbruck, Austria, 17-21 March 1975.

E. L. Petersen and N. O. Jensen, A Mesoscale Phenomenon Revealed by an Acoustic Sounder. Workshop on Urban and Mesoscale Meteorology, Nordforsk, Uppsala, Sweden, 7-9 October 1975.

B. D. Rainford, B. Buras, and B. Lebech, Inelastic Neutron Scattering from Cerium under Pressure. 21st Annual Conference on Magnetism and Magnetic Materials, Philadelphia, Pennsylvania. 8-12 December 1975.

O. Rathmann, Crystal Fields in Diluted Er and Dy Alloys Measured by Inelastic Neutron Scattering. Danish Society for the Physics and Chemistry of Condensed Matter. General meeting, Rungsted, 20-22 May 1975.

H. Sørensen, Secondary emission from Solid Deuterium. Danish Society for the Physics and Chemistry of Condensed Matter. General meeting, Rungsted, 20-22 May 1975.

H. Sørensen, On the Emission of Secondary Electrons from Solid Deuterium. 6th International Conference on Atomic Collisions in Solids, Amsterdam, The Netherlands, 22-26 September 1975.

Degrees, Students, etc.

During the period under review one member of the staff acquired the following degree:

Klaus Hedegaard	cand. scient.

The following postgraduate students carried out research at the Physics Department leading to the degree of lic. techn. or lic. scient. (corresponds to Ph.D.):

Peter Aarosiin Hansen	(Solid State Physics)
Jørgen Højstrup	(Meteorology)
Niels Otto Jensen	(Meteorology)
Leif Wagner Jørgensen	(Plasma Physics)
Jens Juul Rasmussen	(Plasma Physics)
Ole Rathmann	(Solid State Physics)

The following students from Danish universities worked on Master's thesis projects at the department:

Knud Møllenbach	(Solid State Physics)
Flemming Thomsen	(Plasma Physics)

During January and August 1975 students from the Universities of Århus and Copenhagen took part in the following laboratory courses organized by staff members:

1) Neutron Scattering	(P. Aarosiin Hansen O. Rathmann and E. Warming)
2) Plasma Physics	(P. Michelsen and H. L. Pécseli)

Three foreign students sponsored by the IAESTE carried out practical work at the department as part of their general training.

7. STAFF OF THE PHYSICS DEPARTMENT

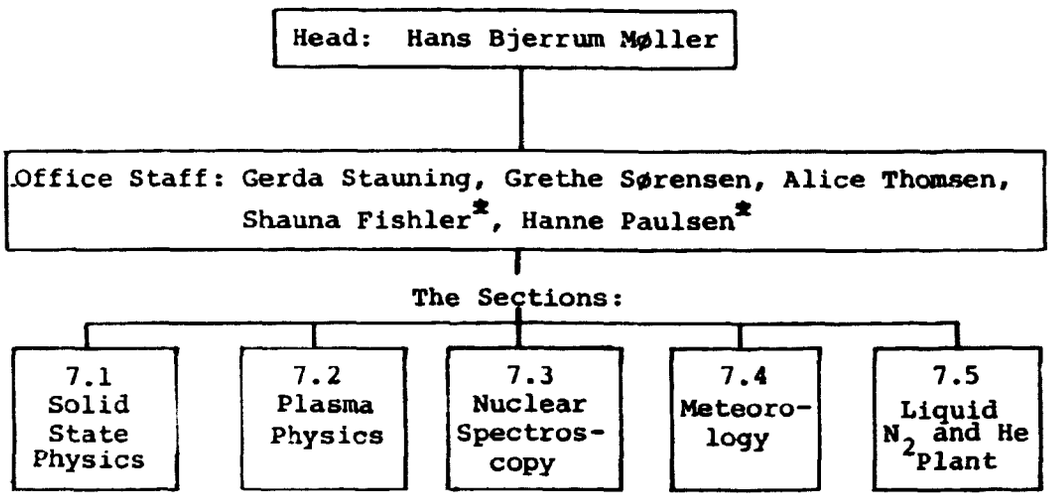

7.1 Solid State Physics

Scientific Staff	Technical Staff
Jens Als-Nielsen	Bjarne Breiting
Ove W. Dietrich	Kaj Christensen
Jens Gylden Houmann	Arent Hansen
Ove Jepsen*	Bent Heiden
Jørgen Kjems	John Z. Jensen
Bente Lebech	Louis G. Jensen
Per-Anker Lindgård	Steen Jørgensen
Knud Møllenbach*	Werner Kofoed
Hans Bjerrum Møller	Jens Linderholm
Mourits Nielsen	Jørgen Munck
Elisabeth Warming	Allan Thuesen
	Sven Aaen-Larsen*

*) Temporary assistant

Consultants

Ole Krogh Andersen[+]
Bronislaw Buras[++]
Rodney M. J. Cotterill[+]

Post Graduate Students

Peter Aarosiin Hansen[+]
Ian Utke Heilmann[++]
Jens Klæstrup Kristensen[+]
Ole Rathmann[+]

Long Term Visitors

Mansoor M. Beg[**],	Pakistan Institute of Nuclear Science and Technology, Pakistan
John Cooke,	Oak Ridge National Laboratory, Tennessee, USA.
William D. Ellenson,	University of California, California, USA
Janos Kollar[**],	The Central Research Institute of Physics, Budapest, Hungary
Uffe K. Poulsen,	IS Datacentralen, Copenhagen (on leave)

Short Term Visitors

W.J.L. Buyers,	Chalk River Nuclear Laboratories, Canada
R. A. Cowley,	University of Edinburgh, Scotland
J. Damgård,	University of Copenhagen, Copenhagen
H. Fogedby,	Institute Laue-Langevin, Grenoble, France
M. Hauschult,	University of Copenhagen, Copenhagen
W. Hayes,	Oxford University, U.K.
A. Kowalska,	Jagiellonian University, Cracow, Poland
A. Luther,	Harvard University, Massachusetts, USA
B. Lüthi,	Rutgers University, New Jersey, USA
G. A. Mackenzie,	University of Edinburgh, Scotland
G. M. Meyer,	University of Edinburgh, Scotland
G. S. Pawley,	University of Edinburgh, Scotland
P. Platzman,	Bell Laboratories, New Jersey, USA
B. D. Rainford,	Imperial College, London, U.K.
T. Riste,	UFA, Kjeller, Norway
K. Ziebech,	Institute Laue-Langevin, Grenoble, France

[+] From the Technical University of Denmark

[++] From the University of Copenhagen

[**] IAEA fellow

7.2 Plasma Physics

Scientific Staff

Che-Tyan Chang**
Vagn O. Jensen
Poul Michelsen
Per Nielsen (from Sept. 1)
Hans Pécseli
Alfred H. Sillesen
Hans Sørensen
Flemming Øster (until Jan. 31)

Technical Staff

Bengt Hurup Hansen
Mogens Nielsen
Arne Nordskov
John Petersen
Børge Reher
Hans Skovgård

Consultants

Nicola D'Angelo++
Chang Mou Tchen+++

Post Graduate Students

Leif Wagner Jørgensen+
Jens Juul Rasmussen+

Short Term Visitors

D. Dimock, Princeton University, New Jersey, USA
N. Sato, Tohoku University, Sendai, Japan

7.3 Nuclear Spectroscopy

Scientific Staff

Verner Andersen
Carl Jørgen Christensen

Technical Staff

Paul Andersen
Finn Hansen

** On leave at the Max-Planck-Institute, Garching, Germany
+ From the Technical University of Denmark
++ From the Danish Space Research Institute
+++ From the City University of New York, USA

7.4 Meteorology

Scientific Staff	Technical Staff
Niels E. Busch	Jørgen Christensen
Klaus Hedegaard*	Gunner Dalsgaard
Leif Kristensen	Morten Frederiksen
Søren E. Larsen	Gunnar Jensen
Erik Lundtang Petersen	Knud Sørensen

Consultants	Post Graduate Students
Peter Dorph-Petersen++	Jørgen Højstrup+
Chan Mou Tchen+++	Niels Otto Jensen+

Long Term Visitors

Ole Christensen,	ISVA, The Technical University of Denmark

Short Term Visitors

J. A. Dutton,	Pennsylvania State University, Pennsylvania, USA
H. A. Panofsky,	Pennsylvania State University, Pennsylvania, USA
E. W. Peterson,	Oregon State University, Oregon, USA
D. W. Thomsen,	Pennsylvania State University, Pennsylvania, USA

7.5 Liquid N_2 and He Plant

Technical Staff
John Z. Jensen
Erik Knudsen
Bent Ferdinansen**

---

* Temporary assistant

** Part time assistant from the Risø Service

\+ From the Technical University of Denmark

++ From the Danish Meteorological Institute

+++ From the City University of New York, USA

ISBN 87 550 0368 0